

Pulsed Flow Wave Attenuation on a Regulated Montane River

By

CATHERINE SAYAKA FONG

B. S. (Leland Stanford Junior University) 2009

THESIS

Submitted in partial satisfaction of the requirements for the degree of

MASTER OF SCIENCE

In

Hydrologic Sciences

in the

OFFICE OF GRADUATE STUDIES

of the

UNIVERSITY OF CALIFORNIA DAVIS

Approved:

Joshua H. Viers, Chair

Jeffrey F. Mount

Bassam A. Younis

Committee in Charge

2014

Table of Contents

| | |
|------------------------|----|
| Abstract..... | 1 |
| Introduction..... | 3 |
| Methods | 9 |
| Results | 19 |
| Discussion | 27 |
| Conclusion | 31 |
| Acknowledgements | 32 |
| References | 33 |
| Appendix A | 47 |
| Appendix B | 52 |

List of Figures

| | | |
|----------|--|----|
| Figure 1 | Study reach and the Tuolumne River subwatershed | 9 |
| Figure 2 | Longitudinal elevational profile of the study reach. Distance measured from Holm Powerhouse | 10 |
| Figure 3 | Diagram of the method used to identify pulsed flow event boundaries. Note how half day Q_{\min} could differ during the same day. As in the example to the right, often changes in half day Q_{\min} signified long-term changes in baseflows. If the elevated or decreased half-day Q_{\min} value lasted less than 24 hrs, intervening pulses were combined into one pulse during manual adjustment | 12 |
| Figure 4 | Statistical loadings for the first three principal components (PCs) and corresponding shape categories based on a positive or negative correlation are shown for 2008, a year which was representative of the same three patterns found each year of the analysis | 19 |
| Figure 5 | Timing of pulsed flow shape types. Note how front step types are most frequent in the spring and summer when recreational flows occur | 22 |
| Figure 6 | Results from 1D modeling of rectangular pulses showing how duration affects the ΔQ_{tot} , Δz_{tot} , and rising and falling ramping rates ($\Delta z/t$) at two downstream points in the river (Clavey and Turnback; recall that no validation exists on model results at Turnback). Two baseflows ($5 \text{ m}^3/\text{s}$ and $27 \text{ m}^3/\text{s}$) and two initial ΔQ_{tot} ($9 \text{ m}^3/\text{s}$ and $22 \text{ m}^3/\text{s}$) were modeled | 24 |

| | | |
|-----------|--|----|
| Figure 7 | Results from 1D modeling of front step, back step ($\times 2$), goalpost, and tower-shaped pulsed flows. On each x-axis, two pulses were modeled (solid and dashed - - - lines) with different representative magnitude indices. Hydrographs for three locations in the river are shown (see Fig. 1) and measurements of duration, ΔQ_{tot} , and $\Delta z/t$ are provided for two..... | 26 |
| Figure 8 | The following figures represent Principal Component loadings shown by year. Within each year, principal components ordered by % of variance explained. On the x-axis, 0 – 300 was a duration descriptor in which 0 was the beginning and 300 was the end of the event | 47 |
| Figure 9 | Further comparison of observed data and modeled data from the validation run. Specifically, a graphical comparison from a portion of the validation time period and a comparison of stage change. Note that the model overpredicts the stage change for pulsed flows released from both turbines, while it underpredicts stage change for smaller releases..... | 52 |
| Figure 10 | Comparison of observed data and modeled data from the validation run (stage change and slope of falling limb) | 52 |
| Figure 11 | Comparison of observed data and modeled data from the validation run (duration and time of arrival)..... | 53 |

List of Tables

| | | |
|---------|---|----|
| Table 1 | Summary statistics for the shape categories. Although discharge ratios are high, one should note that these data are from Cherry Creek before it flows into the Tuolumne River. Recalculating the discharge ratio for the rectangular shape, for example, adding on the Tuolumne River's 50% exceedance value, produces a much lower mean discharge ratio of 3.3..... | 21 |
| Table 2 | Characteristics of pulses used in the study. The amount of bottom step discharge was calculated by subtracting the volume of the top step from the total volume of the pulsed flow, then calculating the mean bottom step discharge needed to create a pulsed flow with the correct total volume..... | 23 |

Pulsed Flow Wave Attenuation on a Regulated Montane River

Abstract

A major benefit of hydroelectric power generation is its ability to respond quickly to changing power demands through the release of stored water through turbines. However, the abrupt changes in discharge caused by this practice can have detrimental environmental effects downstream, including disruption of aquatic insect communities and stranding of fishes. This study investigated the effects of hydrograph shape on attenuation of regulated pulsed flow events by first categorizing and then modeling the downstream movement of representative pulses on the upper Tuolumne River below Holm Powerhouse in the Sierra Nevadas of California. This water conveyance and hydropower generation system is managed by a public utility and produces flow pulses primarily for hydroelectricity generation and/or downstream whitewater recreation. Operations are highly influenced by a system-wide "Water First" policy, which prioritizes drinking water storage, delivery and quality over other beneficial uses. Pulses are therefore associated with a spectrum of time scales, from predetermined schedules decided far in advance to hydropeaking operations responding to current demands. We extracted underlying hydrograph shape patterns using principal component analysis on individual pulsed flow events released from 1988-2012 (n=4439). From principal component loadings, six shape categories were determined: rectangular, front-step, back-step, goalpost, centered tower, and other. The rectangular and stepped shapes were the most frequent, composing 62% and 24% of total events, respectively. The rectangular shape was often

produced by “standard” recreational pulsed flow releases during the summer, while the stepped shapes were often used during times of system-wide water conservation or were recreational flows bordered by periods of elevated flows. The stepped shape increased in occurrence after the "Water First" policy took effect in 1993 and dominated two drier years (2007 and 2009). After categorization by shape, magnitude and durational indices were used to construct representative pulsed flow events. Attenuation of these representative pulses was then modeled using a 1D hydraulic model of 42 river km prepared in HEC-RAS. As no ramping rate restrictions or physical structures meant to alter pulsed flow propagation downstream exist within the system, natural attenuation was the only potential major modifying agent. However, model results demonstrated a clear durational threshold for representative pulses (~ 3-5 hours) over which the degree of attenuation of ramping rates and peak discharge approached a limit. These thresholds were unique to the study reach and were dependent upon river morphology, bed characteristics, and flow rates. Simulations of front and back-step representative pulses showed trade-offs between attenuation of peak magnitudes and steepness of rising ramping rates. Reshaping pulses to be reduce the adverse ecological effects of rapid changes in stage and velocity at all points downstream was infeasible if the system was required to maintain current electricity production and recreational service levels.

Introduction

Hydroelectricity is a major component of the world's energy portfolio, now supplying approximately 16% of the world's electricity (OECD/IEA, 2010). However, flow modifications caused by river impoundments are a major cause of a steep decline or complete loss of freshwater species (Bunn and Arthington, 2002; Dudgeon *et al.* 2006). Compromises between human needs and freshwater ecosystem health are increasingly sought (Le Quesne *et al.* 2010); in the case of hydropower projects, these compromises often involve modifications to downstream releases (Richter and Thomas, 2007). Hydropower generation often produces periodic below-bankfull flow pulses of discharge from reservoirs on a demand basis, with additional release pulses to meet other objectives, such as recreation, sediment flushing, or water deliveries. Since hydropower plants are typically able to respond quickly to changing electricity loads, hydroelectricity is often used as peaking power in order to take advantage of higher prices for electricity when demand is high, and production closely follows periods of demand (Jager and Bevelhimer, 2007). These rapidly fluctuating flow releases are called hydropeaking flows, and corresponding changes in discharge often occur on an hourly or daily basis.

Detrimental effects of pulsed flows to downstream ecosystems come from both rapid changes in discharge (increase and decrease) and changes in stream temperature. The changes in discharge create a hydrodynamic wave (Ferrick, 1985) as well as a concomitant thermal wave of warmer or cooler water that propagates downriver (Frutiger, 2004; Toffolon *et al.* 2010) often with a different celerity (Zolezzi *et al.* 2011). In some water systems, natural attenuation

is expected to dampen flow pulses until they cause minimal effects to downstream biota. Attenuation of pulses involves decreases in hydraulic variables such as Q_{peak} , rising and falling ramping rates, and wave celerity. However, attenuation rates are unique to different river systems with varying river morphology and bed characteristics; increased channel complexity, riparian vegetation, channel connection to the floodplain, and decreased channel slope are acknowledged to contribute to attenuation (Campbell *et al.* 1972; Liu *et al.* 2004; Sholtes and Doyle, 2011; Hauer *et al.* 2012).

Quantifying impacts of pulsed flows in river systems necessitates quantitative descriptive measures of pulsed flow releases and overall operations. This can be difficult as pulsed flow operations, especially when used for hydropeaking, are acknowledged to cause extremely irregular flow releases, often producing pulses with multiple steps or peaks. In river modeling studies, pulsed flows are often modeled with simple rectangular shapes. In this scenario, discharge rises at a constant rate to a certain value. This value is held for a period of time, then discharge decreases at a constant rate. However, the varied shape (the shape as seen on a hydrograph) of pulses also affects attenuation by, in simplified terms, redistributing the inertia and pressure gradients within the wave (Sturm, 2001). If modeling exercises based on rectangular releases are used to define operational rules when other shapes attenuate much differently in the river, the original intent of the operational constraint can be undone.

This study sought to classify common pulsed flow shapes in the Tuolumne River, located in the California Sierra Nevadas, and model the attenuation of representative pulsed flows. Pulsed flows in this system were generally produced for electricity generation, recreation, and water delivery. The study hypothesized that patterns in pulsed flow shapes could be detected in

the historic discharge record, and that common pulsed flow releases would attenuate differently such that some releases would have lesser effects on biota downstream. This study identified 4439 pulsed flow events and analyzed these events using Principal Component Analysis (Jolliffe, 2002) to isolate representative pulsed flow shapes. The attenuation of these shapes downriver was then quantified using a one-dimensional hydraulic model of the study reach. Differences in attenuation caused by pulse shape were observed.

Effects on Abiotic and Biotic Factors

Although the effects of pulsed flow regimes on downstream ecosystems are site-specific, some broad similarities can be drawn between effects in different streams and rivers. Pulsed flows cause physical habitat alterations on both short and long-term scales. During the course of a pulse, suitable habitat for organisms is expanded or contracted through changes in microhabitat variables such as water depth, bed surface area, and velocity (Cowx *et al.* 1998). Long-term changes in morphology can result from the pulsed flow regime and other impacts from dam operations, which often include the stabilization of flows such that fewer high and low flow events occur and a decrease in the sediment load of the water released from the dam (Grant *et al.* 2013). These changes can include the homogenization of morphological features, including aggradation of pools and absence of pool-riffle sequences, erosion from channels, vegetation of gravel bars, and creation of fine sediment berms bordering channels (Moog, 1993; Sear, 1995; Fette *et al.* 2007). Substrate composition can also be affected by pulsed flow

regimes, with common effects including increased fines and bed armouring, resulting reduced vertical connectivity (Harby and Noack, 2013).

Pulsed flow regimes are associated with a number of detrimental effects on downstream biota (Cushman, 1985). Numerous studies, mainly in Europe and the United States, have found different combinations of reduced diversity, biomass, and richness of benthic species and changes in community trophic structure resulting from hydropeaking operations (Bain, 2007), with impacts falling heavily on sensitive species (Richards *et al.* 2013). Increased drift from both temperature and discharge changes may cause substantial losses to benthic populations (Cereghino and Lavandier, 1998; Bruno *et al.* 2010; Bruno *et al.* 2012). Some studies have found that impacts are more or only severe within the zone of shoreline that is frequently dewatered during pulse flow events (Troelstrup and Hergenrader, 1990; Harby *et al.* 2001) and that impacts on benthic populations may decrease with further distance from the dam (Camargo and Voelz, 1998).

Adverse effects of pulsed flow regimes on individual fish include downstream displacement, stranding, reduced spawning success, nest site dewatering, reduced rearing survival, and altered migration (Young *et al.* 2011). Behavioral responses by fishes, such as avoidance, are often energetically costly (Scruton *et al.* 2008). A large amount of attention in the literature focuses on stranding, mainly of juvenile and adult salmonids. Stranding rates are impacted by physical factors such as the shoreline slope, water temperature, ramping rates, water quality, seasonality, time of day, and base discharge (Nagrodski *et al.* 2012). Age and species type influences susceptibility, with eggs and early life stages being particularly vulnerable (Saltveit *et al.* 2001). River morphology also affects stranding rates. Side channels

and backwater areas, which become disconnected after pulses, as well as gravel bars, large debris, cobble bars, and potholes are all potential stranding sites (Bradford, 1997; Bell *et al.* 2008; Nagrodski *et al.* 2012).

Amphibians are also impacted by the rapid depth and velocity changes caused by pulsed flows. Perhaps the best studied of these species, with respect to hydropeaking in Sierra Nevada rivers, is the river breeding foothill yellow-legged frog (*Rana boylei*). Their egg masses and tadpoles are especially vulnerable to rapid shifts in velocity and changes in depth (Kupferberg, 2009; Yarnell *et al.* 2012). Pulsed flows may cause entrainment or cause long periods of sheltering, decreases in size, later development, and increased predation (Kupferberg *et al.* 2011).

Mitigation Measures

Mitigation for adverse biotic and abiotic impacts of pulse flows fall under three categories: operational, structural, and morphological measures. Operational changes are commonly built around the identification of important abiotic thresholds or cues to species-specific behavioral responses and life history events (Lytle and Poff, 2004; Yarnell *et al.* 2010). Current operational mitigation measures include constraints on ramping rates (Halleraker *et al.* 2003; Smokorowski *et al.* 2011), seasonal and/or diel shifts in operation, and decreasing the discharge ratio or drawdown range (Q_{\max}/Q_{\min}), often by increasing base flows (Cowx *et al.* 1998). However, many links between flow variables and specific biotic response are not well understood and any links that have been established have site-specific threshold values for

impacts. In some cases, negative effects may not correlate to a simple rate-of-change or flow magnitude shift but to specific discharge changes at certain flow levels (Tuhtan *et al.* 2012). The well-accepted natural flow regime framework (Poff *et al.* 1997) is difficult to adapt into a flow regime on regulated rivers, and rivers with pulsed flow regimes are especially challenging (Jones, 2013). Most current methodologies to evaluate impacts do not take into account frequent rises and falls in flow, which is a defining feature of the pulsed flow regime (Morrison and Smokorowski, 2000).

Additionally, implementing suggestions for environmental operating constraints often mean alterations and/or decreases to current levels of electricity production and other ecosystem services such as irrigation diversions and recreation flows. For example, many hydropower dams have minimum flow requirements but fewer have ramping rate restrictions. Ramping rate constraints can significantly affect hydropower profits, although the degree of impact depends on the severity of the ramping rate constraint (Niu and Insley, 2013). Suggestions of strict ramping rate restrictions for certain species can be assumed to impact hydropower production. For instance, Rood *et al.* (1998) suggest that during cottonwood recruitment season, down-ramping rates of less than 2.5 cm/day be used to aid cottonwood seedling recruitment in the Western United States. Kupferberg *et al.* (2011) recommend curtailing pulsed flow production during breeding and metamorphosis of foothill yellow-legged frogs (*Rana boylei*) in certain Sierra Nevada rivers from spring to fall. To prevent stranding of juvenile salmonids, downramping rates of approximately less than 10 cm/hr as well as dewatering at night have been suggested in Canada and Norway (Bradford *et al.* 1995; Halleraker *et al.* 2003).

The remaining two categories of mitigation measures encompass activities such as installation of in-stream structures that detain and dampen flows, diversions of outflow into a lake or reservoir and in-stream compensation basins, and morphological measures such as physically changing river width and roughness (Renöfält *et al.* 2010). A recent study by Person *et al.* (2013) compared mitigation measures for an alpine river with reaches of varying morphologies, ranging from a simple, single channel reach to braided channels. The study found that structural, as opposed to operational measures, provided the best cost-benefit ratio when assessed for fish habitat improvement.

Methods

Study Site

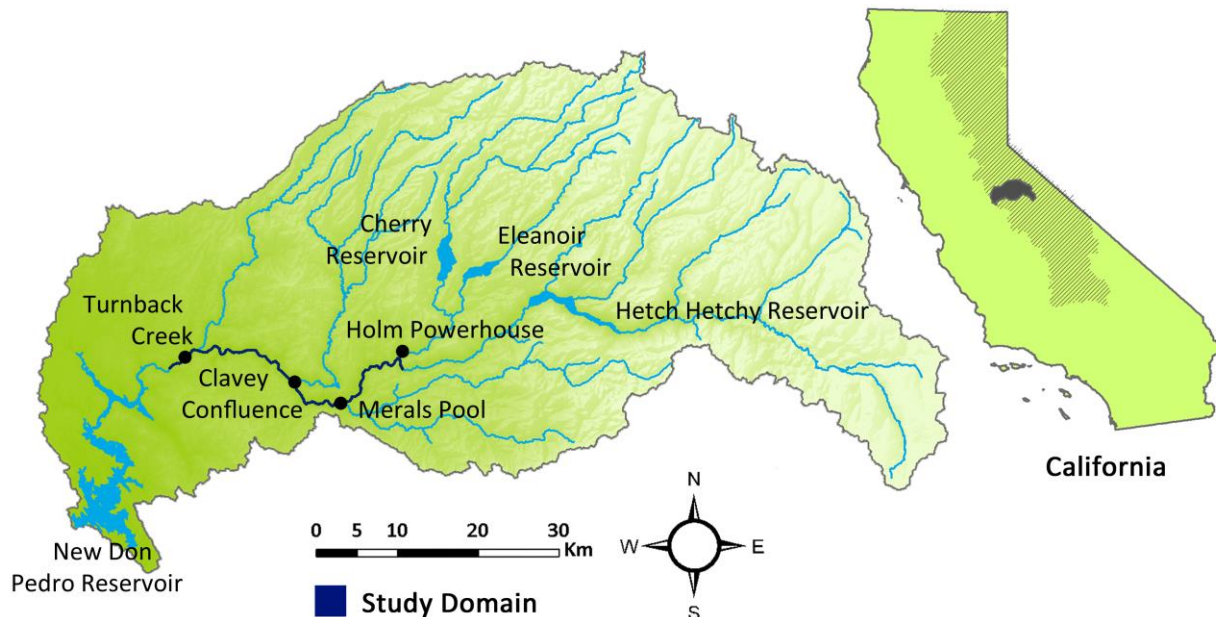


Figure 1 : Study reach and the Tuolumne River subwatershed.

The study reach (Fig. 1) is a 42.1 km stretch of the mainstem Tuolumne River (downstream of 37°52'35"N, 119°58'2"W,) and 1.1 km of Cherry Creek (downstream of 37°53'46"N, 119°58'6"W) between Holm Powerhouse and New Don Pedro Reservoir (storage capacity $2.5 \times 10^9 \text{ m}^3$). The river segment studied is a confined, steep-gradient, bedrock channel with numerous step-pools and boulder cascades.

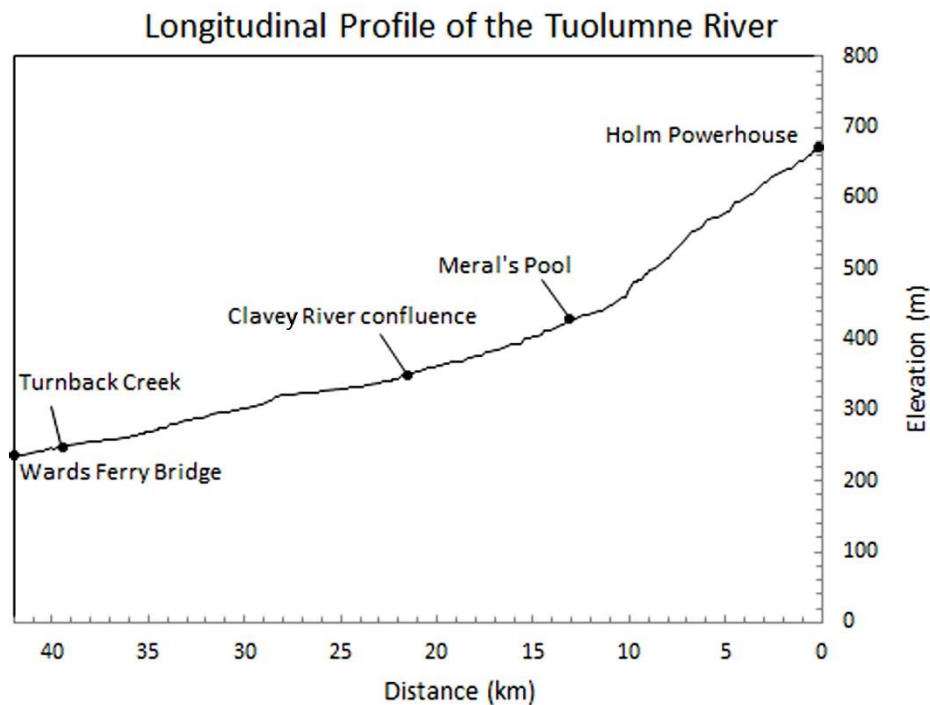


Figure 2: Longitudinal elevational profile of the study reach. Distance measured from Holm Powerhouse.

Below Meral's Pool (see Fig. 2) the channel slope noticeably flattens and contains increasingly long stretches of deep bedrock channel. The river terminates in New Don Pedro Reservoir. The drainage area above New Don Pedro Reservoir is 3970 km^2 and the elevation ranges 236-3990 m. The upper 40% of the watershed is contained within Yosemite National Park, with the middle elevations mainly consisting of public lands and the lower elevations of

private land. The majority of the watershed above the study area consists of granitic bedrock covered with a thin soil layer.

The study reach is part of the Hetch Hetchy Water and Power System, which is administered by the San Francisco Public Utilities Commission (SFPUC). Infrastructure was first built in the early 1900s to provide drinking water to San Francisco and surrounding cities (Hundley, 1992). This controversial development included construction of O'Shaunnesy Dam which inundated Hetch Hetchy valley in Yosemite National Park (Null and Lund, 2006). The water system now includes multiple reservoirs in both the Sierra Nevada and the San Francisco Bay Area. Since 1993 SFPUC has adopted a "Water First" policy, which prioritizes drinking water supply and quality over other uses (San Francisco Planning Department, 2008).

The pulsed flows used in this study are generated by Dion R. Holm Powerhouse, which is fed by Cherry Reservoir (storage capacity of $3.4 \times 10^8 \text{ m}^3$) and Eleanor Reservoir ($3.3 \times 10^7 \text{ m}^3$), with releases into the mainstem Tuolumne River via Cherry Creek. Holm Powerhouse contains two six-jet Pelton-type impulse turbines with a maximum generating capacity of ~170 MW. When both turbines are running at full power, approximately $28.3 \text{ m}^3/\text{s}$ is released from the powerhouse. Releases from the upstream Hetch Hetchy Reservoir are not pulsed flow events, as water is diverted via the Canyon Power Tunnel and Mountain Tunnel for drinking water delivery and off-channel power production at Kirkwood and Moccasin Powerhouses. SFPUC manages Holm Powerhouse concurrently with these two other powerhouses, and therefore operations are also dependent on demand load and combined generation. At Holm Powerhouse, hydropeaking occurs throughout much of the year, with summer peaking

schedules shifted to prioritize provision of recreational flows. Currently there are no regulatory ramping rate restrictions for operations on this system.

Runoff is driven by a Mediterranean climate, causing the majority of precipitation to fall in the winter, which in unimpaired conditions leads to a gradual spring snowmelt recession and low summer baseflows. The quantity and distribution of precipitation have high inter-year variability (Null and Viers, 2013). After impoundment, the mean annual discharge in Cherry Creek below Holm Powerhouse is $20 \text{ m}^3/\text{s}$ with a 50% exceedance probability at $17 \text{ m}^3/\text{s}$ (USGS, 2013a), while the mean annual discharge of the mainstem Tuolumne River above the confluence of Cherry Creek and Tuolumne River is $16 \text{ m}^3/\text{s}$ with a 50% exceedance probability of $4 \text{ m}^3/\text{s}$ (USGS, 2013b).

Identifying Representative Shapes

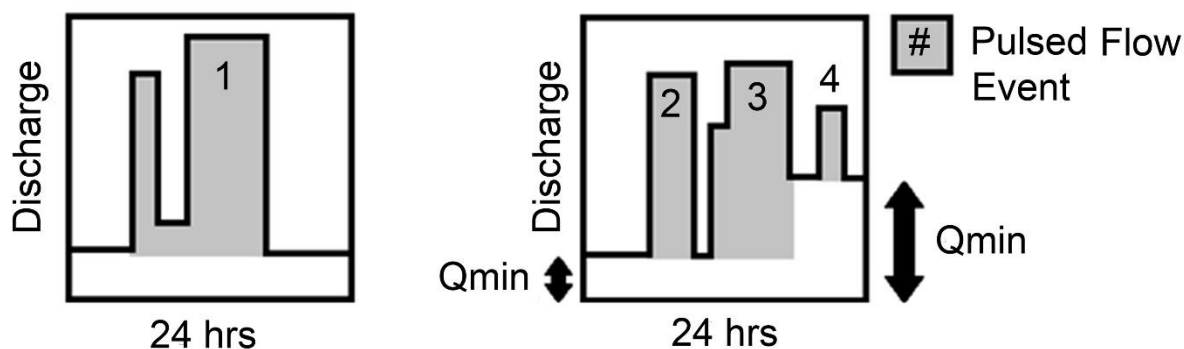


Figure 3: Diagram of the method used to identify pulsed flow event boundaries. Note how half day Q_{\min} could differ during the same day. As in the example to the right, often changes in half day Q_{\min} signified long-term changes in baseflows. If the elevated or decreased half-day Q_{\min} value lasted less than 24 hrs, intervening pulses were combined into one pulse during manual adjustment.

Pulsed flow events were identified from 15-minute discharge data spanning 1988-2012 ($n=4439$) from USGS gage No. 11278400, located approximately 0.8 km downstream of the tailrace of Holm Powerhouse. For the purposes of this study, boundaries of flow events were identified from when rates of change exceeded a certain threshold ($\Delta 0.14 \text{ m}^3/\text{s}/15 \text{ min}$) and discharge rates were either departing from or returning to the half-day minimum discharge value (Q_{\min}). Therefore, single events could encompass multiple discharge spikes if each one did not fully decrease to Q_{\min} (see Fig. 3). This method was made more robust since operations were normally run on a diel basis. Event boundaries were manually examined and spikes potentially driven by natural rain or snowmelt events were removed from the dataset.

Principal component analysis (PCA) was then used to identify representative pulsed flow shapes. PCA is a statistical technique that produces a small set of uncorrelated vectors, or principal components (PC), which are orthogonal and preserve much of the variation within the original multivariate dataset while maintaining its structure (Jolliffe, 2002). PCA has previously been used in hydrological studies to classify diurnal runoff from glaciated catchments (Hannah *et al.*, 2000), to find patterns in water table levels (Winter *et al.*, 2000), and to characterize seasonal changes in dissolved organic matter in glacial melt water (Barker *et al.*, 2009).

Data input matrices were formed for each year of discharge data consisting of n rows of pulsed flow events and m columns of discharge values. The number of columns was increased to at least $n+1$ to calculate a stable covariance matrix. Linear interpolation was used so that each event contained $n+1$ discharge measurements. Events were standardized using z-scores such that the $\mu = 0$ and $\sigma = 1$.

PCA was then run on the standardized data matrices for each individual year.

Histograms of Pearson's correlation coefficients between PC loadings and pulsed flow events were used to determine if individual PC shapes were controlled by the actual shape of a set of hydropeaking events or were instead driven by cumulative variation. The first two PCs and a portion of the third generally contained high r values ($|r| > \pm 0.7$, to select for both strong positive and negative correlations) with groups of actual pulsed flows, indicating that these PCs corresponded to a subset of shapes within the dataset. A cutoff of Pearson's correlation coefficient of ± 0.6 was then used to divide the events into bins containing the individual pulsed flow shapes.

Identification of representative events within each PC category required selection of magnitude indices (duration, Q_{\min} , Q_{\max}) to correspond to each shape category. Using these indices, hierarchical and k-means clustering as well as cluster plots were used in an attempt to group events within each PC category. However, this analysis did not produce clearly defined groupings, potentially due to the highly irregular nature of the pulsed flows themselves. Therefore, in general, events with magnitude indices corresponding to the 25th, 50th, and 75th percentiles of each variable were used to produce representative events. Data was tested for multimodality, and when the data was uni-modal and the median value of an index represented the overall distribution of events well, only the median value was used for modeling exercises.

Hydraulic Modeling

This study used the U. S. Army Corps of Engineers' River Analysis System (HEC-RAS) to model unsteady open-channel flow (USACE, 2010). HEC-RAS is a one-dimensional hydraulic model that uses an implicit finite difference scheme to solve the Saint Venant equations. These equations are comprised of the conservation of mass and conservation of momentum equations

$$(1) \quad \partial Q / \partial x + \partial A / \partial t + \partial S / \partial t - q = 0$$

$$(2) \quad \partial Q / \partial t + \partial (VQ) / \partial x + gA(S_0 + S_f) = 0$$

in which Q = flow, A = cross-sectional area, S = storage, q = lateral inflow, V = velocity, g = gravitational acceleration, S_0 = bed slope, and S_f = friction slope.

Geometric data were taken from high-resolution photogrammetry from airborne surveys of the river canyon conducted in August of 2007 during a low flow period (Towill Surveying, 2007). Individual reaches were classified visually either as a pool, glide, low-gradient riffle, high-gradient riffle, or cascade using a method similar to previous studies of adjacent reaches (Jayasundara *et al.* 2010). In total, 861 cross sections were placed across the river at changes in reach type, noticeable changes in bank width, and sharp bends to capture representative river geometry with minimum cross sections. Bathymetry below the water surfaces was estimated using Manning's equation

$$(3) \quad Q = (1/n)R_h^{2/3}AS_0^{1/2}$$

in which R_h = hydraulic radius and n = Manning's n value. Reach slopes were found from elevations of a streamline drawn over the channel thalweg. Slopes of 0 were changed to 0.0001. Manning's n was estimated using Chow (1959). A trapezoid was inserted at the bottom of the channel to approximate the wetted cross-sectional geometry, with dimensions derived from the calculated cross-sectional area (A) and by setting the width of the longest parallel trapezoid edge equal to the width of visible surface water.

The final model geometry consisted of 1974 cross sections spaced from 6.4 – 303 m apart, with an average spacing of 26 m. Additional cross sections ($n=1113$) were linearly interpolated between measured cross sections as a close spacing was necessary to prevent instabilities within the steep mountainous river. A sensitivity analysis was performed by varying model time steps (10-30 sec), theta values (0.85 – 1.0), and cross section spacing (8 – 30m). Results did not change substantially by changing these parameters, and thus model variables within these ranges were used when possible.

Model Validation

Pulsed flow events in September 2008, July 2009, and August 2009 were used for the validation run by comparing stage results to a 30-min stage data logger in Meral's Pool ($n=56$; unpublished data from SFPUC). The validation run periods were chosen to limit hydrologic inputs from tributaries and groundwater sources. Measured discharge during the validation period ranged from $1.4\text{m}^3/\text{s}$ - $29.7\text{m}^3/\text{s}$.

Model validation parameters were selected using the suggestions of Moriasi *et al.* (2007). These parameters were visual comparison, the Nash-Sutcliffe efficiency (NSE) (Nash and Sutcliffe, 1970), percent bias (PBIAS), and the root mean square error standardized with the standard deviation of observational data (RSR). NSE was 0.97 (acceptable range > 0.5), PBIAS was -0.4 % (acceptable range within $\pm 25\%$), and RSR was 0.16 (acceptable range ≤ 0.7). After the initial validation, additional 15-min. stage data from a pressure transducer was collected further downriver at the confluence with the Clavey River (21 km downriver of release) by the author and University of California, Davis researchers. The model simulations were compared against measurements in May and June of 2013, producing NSE = 0.92, PBIAS = 2%, and RSR = 0.28.

At the Clavey confluence the model results displayed more attenuation than observed. The peaks of model peaks were ~ 0.05 m lower than those observed. During periods when tributary and groundwater input was substantial, clear differences in the timing of the wave emerged. Tributary inputs were ignored for this study as limited flow data existed; however, further studies should consider tributary impacts on the behavior of the pulsed flows.

Modeling of Representative Events

A 5-min time step was used for discharge changes in simulation runs, which slightly underestimated actual unrestricted ramping rates. Two different baseflows were used for rectangular runs based on the 50th and 75th quartile baseflows in Cherry Creek and the mainstem Tuolumne River. These combined baseflows were 5 m³/s and 27 m³/s. The remaining

shapes were investigated only at 5 m³/s. Pulsed flow events were described using four variables: duration (t_{tot}), change in discharge (ΔQ) and stage (Δz), and ramping rates on the rising and falling limbs ($\Delta Q / t$ or $\Delta z / t$) in which $t = 1$ hr to allow for comparison with ecological recommendations and additional studies (Bieri and Schleiss, 2011; Meile *et al.* 2011).

Results

Representative shapes

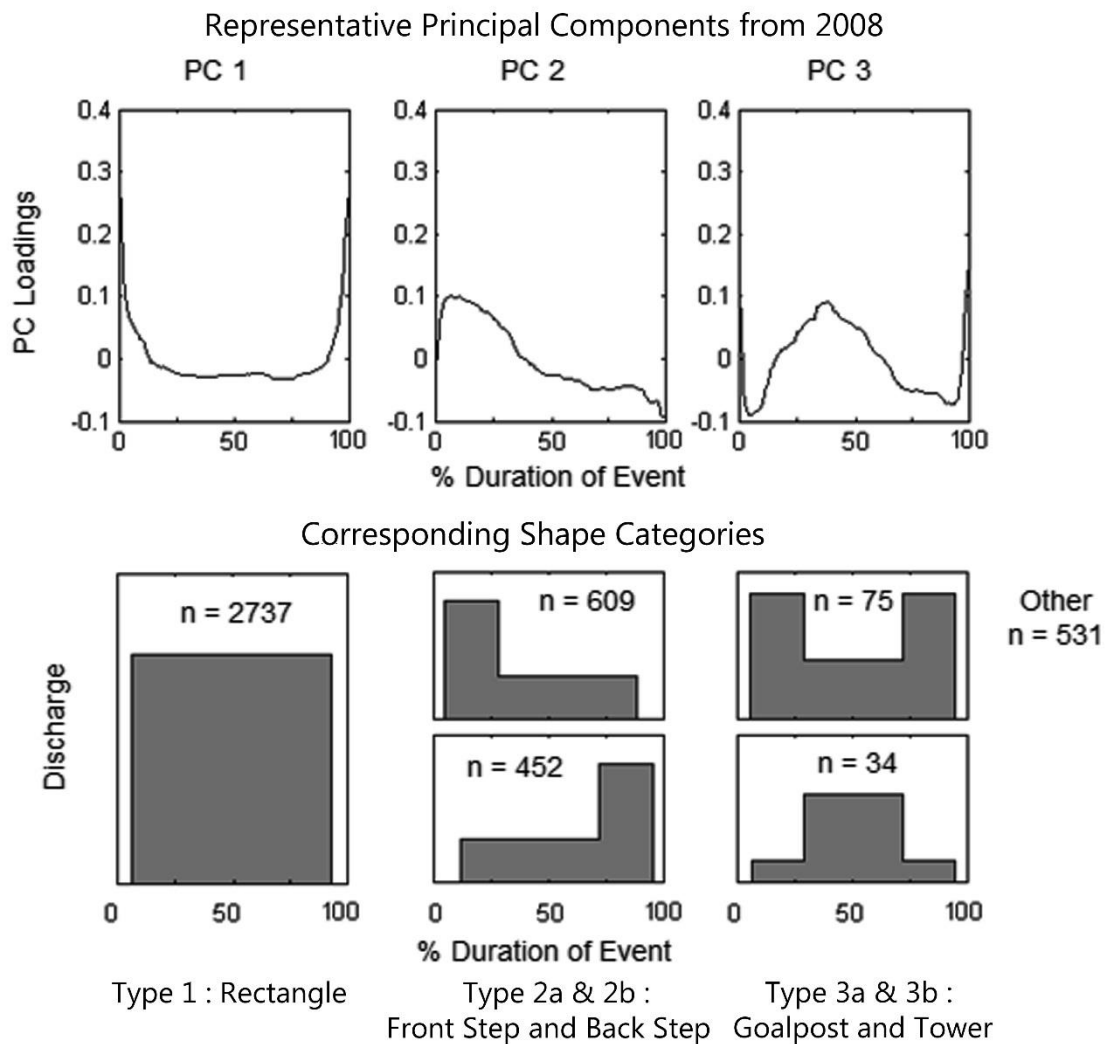


Figure 4: Statistical loadings for the first three principal components (PCs) and corresponding shape categories based on a positive or negative correlation are shown for 2008, a year which was representative of the same three patterns found each year of the analysis.

The pulsed flow events were binned into 6 shape categories, as shown in Fig.4. Although individual years were run separately through PCA, the first three PCs for each year correlated to the same overall shapes (see Appendix A for results from each year).

1. Rectangle (n = 2737): The PC type corresponding to a rectangular shaped pulse explained an average of 50% of the variance within each year. In all but two years this PC type explained the most variation and was the dominant type. The first PC often referred to relative magnitudes of variables (Jolliffe, 2002). In this case, interpreting the PC indicated that most pulsed flow events contained a relatively stationary maximum bordered by a steep increase and decrease. The rectangular shape was considered a “standard” pulsed flow for electricity generation, recreation, and water deliveries.

2a & 2b. Front Step & Back Step (n = 609, n = 452): The second PC, which explained an average of 21% of the variance within each year, had a high correlation with stepped pulsed flows. The loadings for this PC had an offset maximum value that gradually declined on its longest tail, which was interpreted to indicate that many pulsed flow events were not centered and instead peaked either towards the beginning or end of the event.

3a & 3b. Goalpost & Tower (n = 34, n = 75): The third PC, which explained an average of 8% or less of the variance, correlated with either a goalpost or centered tower shape. These types were much less frequent than the other shapes.

4. Other (n = 531): Approximately 12% of pulsed flow events did not fall into the previous 5 categories and were classified as ‘other’.

Summary Statistics

Summary Statistics by Shape Type

| | | Rectangle | Front Step | Back Step | Goalpost | Tower | Other |
|-------------------|--------|-----------|------------|-----------|----------|-------|-------|
| Duration | Median | 17.0 | 16.5 | 19.5 | 16.0 | 16.2 | 17.3 |
| | Mean | 15.6 | 16.2 | 19.3 | 15.1 | 16.3 | 19.0 |
| | Std | 5.9 | 7.5 | 6.5 | 5.1 | 9.5 | 9.0 |
| Minimum Magnitude | Median | 1.5 | 1.7 | 3.4 | 1.2 | 1.9 | 2.4 |
| | Mean | 3.9 | 4.6 | 6.1 | 3.6 | 4.5 | 5.8 |
| | Std | 5.1 | 5.4 | 6.2 | 5.3 | 6.1 | 6.5 |
| Maximum Magnitude | Median | 19.7 | 28.2 | 19.6 | 11.8 | 21.7 | 18.4 |
| | Mean | 19.2 | 25.0 | 19.7 | 14.1 | 22.1 | 20.0 |
| | Std | 9.0 | 8.7 | 9.5 | 8.2 | 9.8 | 9.9 |
| Discharge Ratio | | 12.2 | 12.1 | 10.9 | 10.9 | 10.9 | 11.2 |

Table 1: Summary statistics for the shape categories. Although discharge ratios are high, one should note that these data are from Cherry Creek before it flows into the Tuolumne River. Recalculating the discharge ratio for the rectangular shape, for example, adding on the Tuolumne River's 50% exceedance value, produces a much lower mean discharge ratio of 3.3.

Summary statistics for the different shape categories were provided in Table 1. Both the mean and median duration of events ranged from 15-20 hrs. Although recreational pulsed flows produced in the summer lasted approximately 4 hrs, many of these flows became folded into stepped flows that lasted a longer duration. The data therefore did not contain a clear concentration of pulsed flows of 4-5 hrs duration. The 15-20 hr duration was similar to pulse durations of other hydropeaking operations, such as that of the Noce River in Northern Italy that were found to have common durations of either 5-8 hrs or 15-18 hrs (Zolezzi et al., 2011), corresponding to patterns of electricity prices. Discharge ratios within Cherry Creek had a mean value ranging from 10-12. However, Cherry Creek flowed into the mainstem Tuolumne River only 1.1 km below Holm Powerhouse, which greatly lessened this ratio.

Timing of Pulsed Flow Shape Types

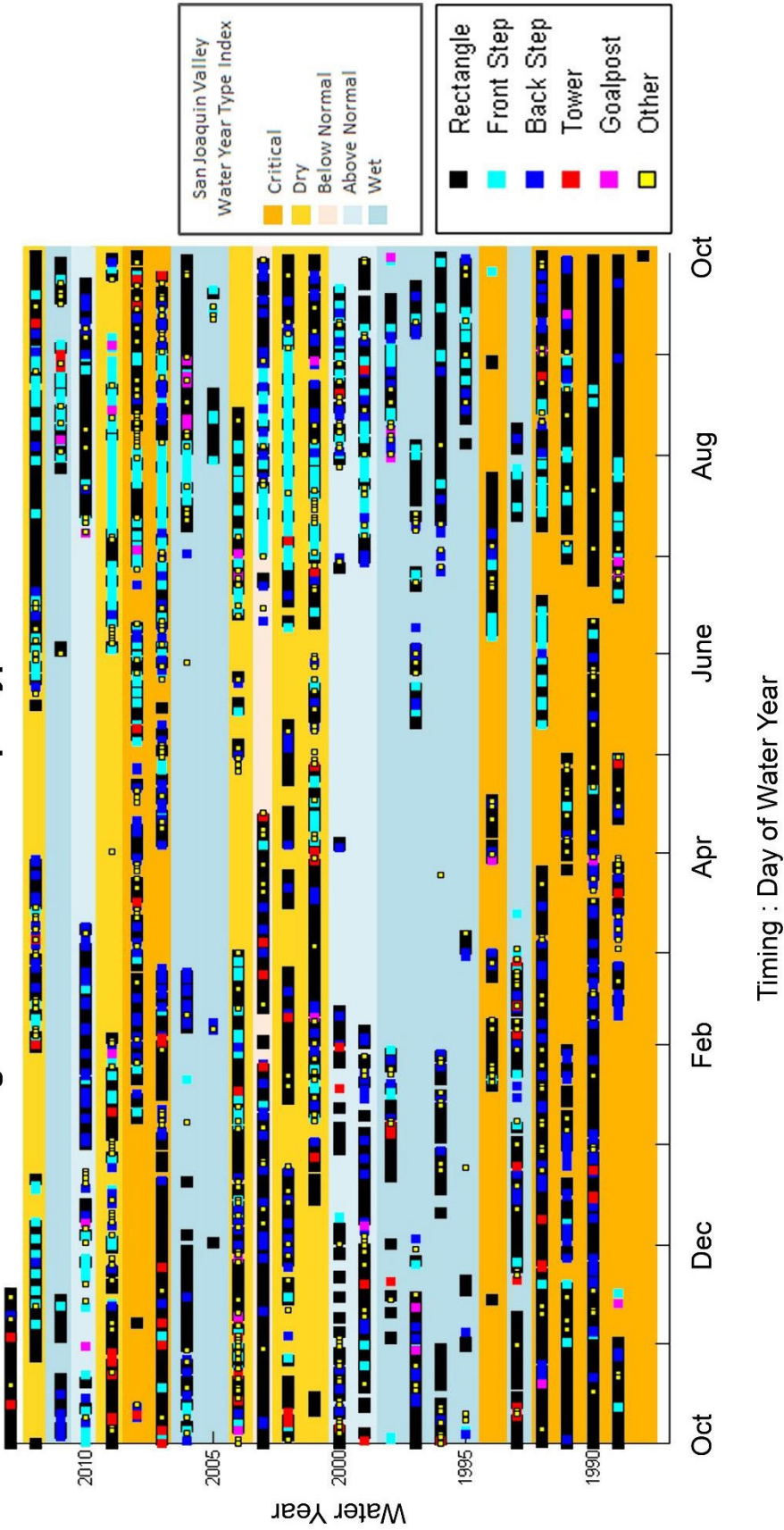


Figure 5 : Timing of pulsed flow shape types. Note how front step types are most frequent in the spring and summer when recreational flows occur.

The timing of the pulsed flow types was plotted in Fig. 5, which showed that pulsed flow events occur year round. Front step flows were concentrated from approximately June to October.

Model Simulations

Model parameters for each of the following types were presented in Table 2. When changes in discharge occurred, ramping rates were modeled as $\Delta Q_{\text{tot}}/5$ min although these discharge changes in actuality occurred more quickly.

Modeled Representative Pulsed Flow Characteristics

| Type | ΔQ_{tot} | $\Delta Q_{\text{lower step}}$ | t_{tot} | t_{peak} |
|--------------------|---|--------------------------------|-------------------|--|
| Rectangular | 9 m ³ /s and 22 m ³ /s (25th and 75th quartile) | - | .5 - 18hrs | t_{tot} |
| Front Step | 15 m ³ /s and 28 m ³ /s (25th and 75th quartile) | 52% of ΔQ_{tot} | 17hrs (median) | 17% of t_{tot} (median) |
| Back Step | 8 m ³ /s and 18 m ³ /s (25th and 75th quartile) | 64% of ΔQ_{tot} | 17hrs (median) | 10% and 43% of t_{tot} (25th and 75th quartiles) |
| Goalpost | 6 m ³ /s and 14 m ³ /s (25th and 75th quartile) | 70% of ΔQ_{tot} | 16hrs (median) | 8% of t_{tot} (average) |
| Tower | 11 m ³ /s and 28 m ³ /s (25th and 75th quartile) | 50% of ΔQ_{tot} | 16hrs (median) | 16% of t_{tot} (average) |

Table 2 : Characteristics of pulses used in the study. The amount of bottom step discharge was calculated by subtracting the volume of the top step from the total volume of the pulsed flow, then calculating the mean bottom step discharge needed to create a pulsed flow with the correct total volume.

Results from the model simulations at Holm Powerhouse, the Clavey River confluence (21 km downstream), and upstream of Turnback Creek (39km downstream, a point near the

reservoir free of its backwater influence) were presented in Figs. 6-7 respectively. These locations represent pool cross sections with comparable widths in order to hold channel geometry constant.

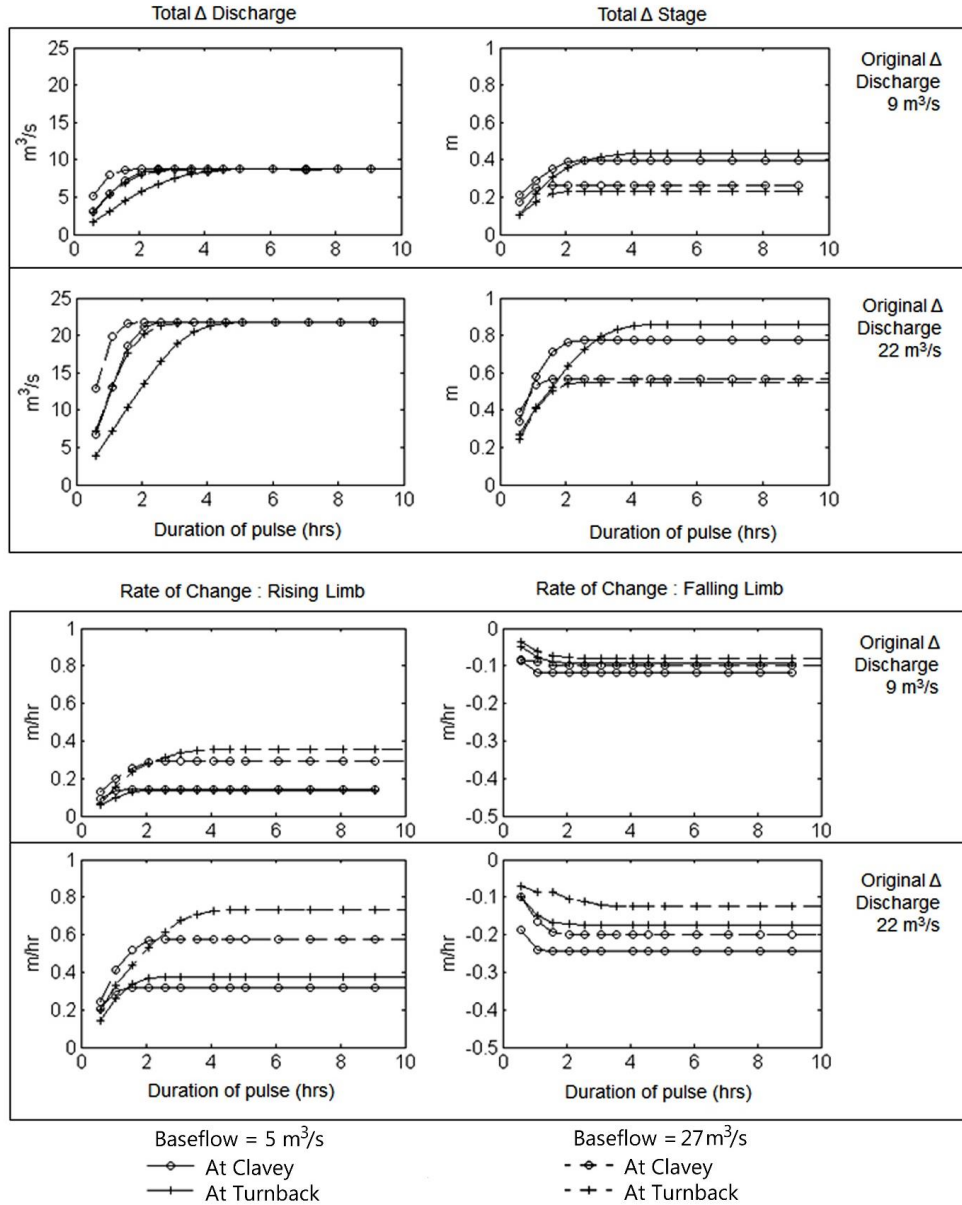


Figure 6 : Results from 1D modeling of rectangular pulses showing how duration affects the ΔQ_{tot} , Δz_{tot} , and rising and falling ramping rates ($\Delta z/t$) at two downstream points in the river (Clavey and Turnback; recall that no validation exists on model results at Turnback). Two baseflows ($5 \text{ m}^3/\text{s}$ and $27 \text{ m}^3/\text{s}$) and two initial ΔQ_{tot} ($9 \text{ m}^3/\text{s}$ and $22 \text{ m}^3/\text{s}$) were modeled.

Rectangular Pulse (Fig. 6) : The results shown for rectangular pulses in Fig. 6 displayed the importance of duration to attenuation behavior downstream. Measures of attenuation – namely the ΔQ_{tot} , total stage change (Δz_{tot}), and $\Delta z/t$ – were shown to move towards a limit as the duration increased. The limits for ΔQ_{tot} , Δz_{tot} , and rising ramping rates were very close to the original measurements at $t = 0$. The falling ramping rates attenuated to a limit which was less steep than at $t = 0$. The ‘durational threshold’ for common discharges on the Tuolumne River was approximately 3 – 5 hrs

2a. Front Step (Fig. 7a) : These modeled stepped shapes, containing just two steps, are representative of the type but do not encompass the full range of variability displayed in the hydrologic record. Stepped shapes often displayed multiple levels of flow between the top and the bottom step and steps were highly irregular. Rising ramping rates steepened slightly in all modeled cases while falling ramping rates decreased in magnitude. The pulses increase in duration by $\sim 30\%$ and lowered in ΔQ_{tot} by $\sim 15\%$.

2b. Back Step (Fig. 7b) : The duration increased by $\sim 20\%$ and the ΔQ_{tot} displayed only a very small decrease if at all. The rising ramping rates remained static, while the falling ramping rates decreased to approximately the same value in all cases (-0.1 m/hr). The behavior of the back step, in contrast with the front step, indicated that the back step had less attenuation of the ΔQ_{tot} , but conversely had less steepening in rising ramping rates. The falling ramping rates for all stepped shapes attenuated to a similar value.

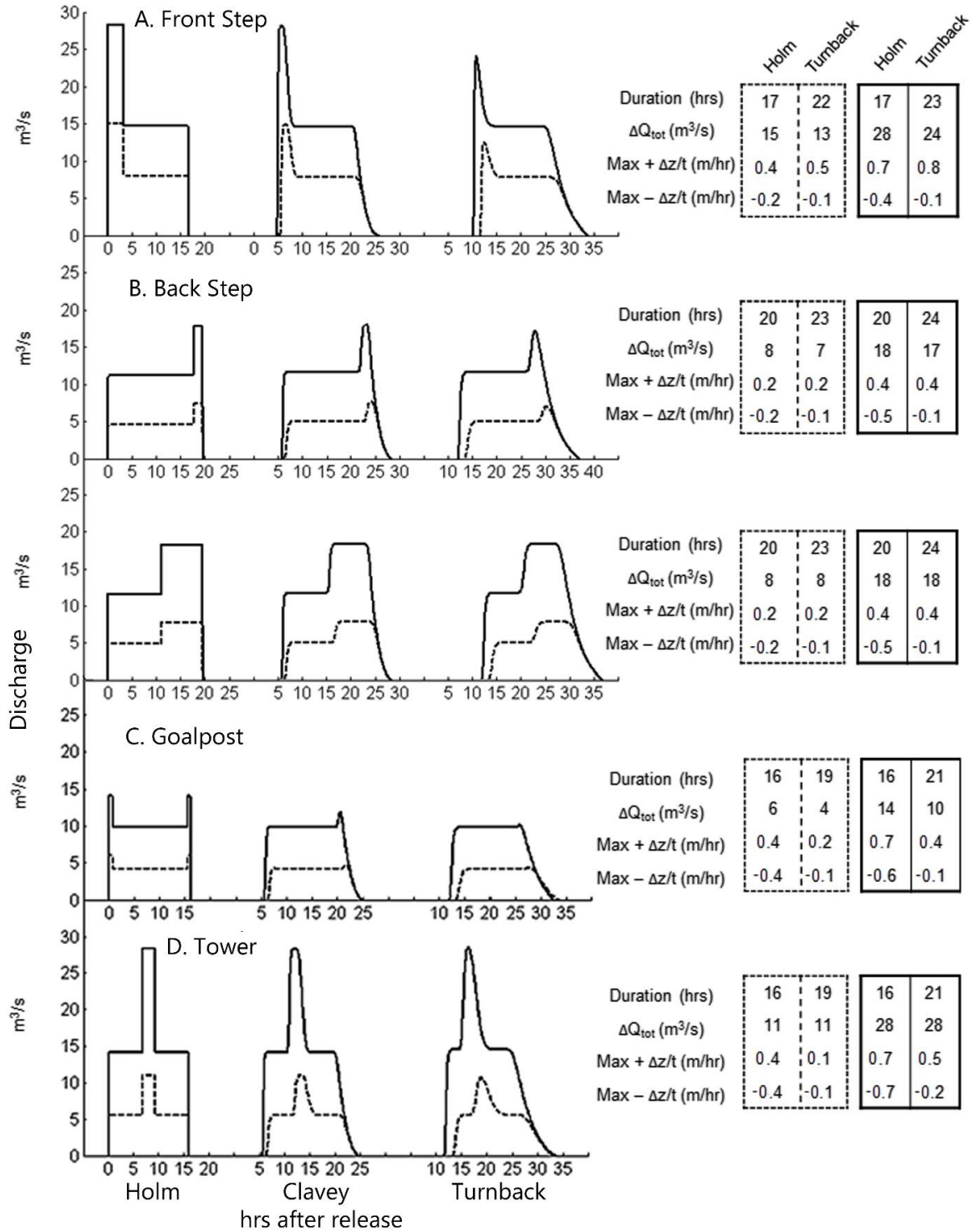


Figure 7: Results from 1D modeling of front step, back step ($\times 2$), goalpost, and tower-shaped pulsed flows. On each x-axis, two pulses were modeled (solid and dashed - - - lines) with different representative magnitude indices. Hydrographs for three locations in the river are shown (see Fig. 1) and measurements of duration, ΔQ_{tot} , and $\Delta z/t$ are provided for two.

3a. *Goalpost (Fig. 7c)*: As shown in Fig. 8, the duration lengthened by 20-30% and the ΔQ_{tot} decreased by $\sim 33\%$. Both rising and falling ramping rates decreased, varying from 50 – 80%.

3b. *Tower (Fig. 7d)* : As shown in the results in Fig. 8, the duration lengthened by 20-30% but the ΔQ_{tot} did not change. Both rising and falling ramping rates decreased, varying from 30 – 80%.

Discussion

Shape Patterns

Although a rectangular shape occurred most frequently in the historic record, other common shapes emerged from this analysis – front and back step, goalpost, and a centered tower shape. As seen in Fig. 5, the timing of the front step indicated its association with recreational boating flows, which take place mainly in the summer. Discharge releases for these rafting flows are usually near turbine capacity. They are released early in the morning, causing any additional releases, often with decreased discharge, to occur in the afternoon. The back step did not display a similar strong pattern.

Additionally, as shown in Fig. 5 by the timing of many stepped and rectangular flows, observed results suggested that pulsed flow types often occur in series, with multiple types occurring one after the other within a given water year. Repeated similar releases indicated that their shape corresponded to specific conditions and/or their accompanying management

strategies. For example, SFPUC's "Water First" policy, and subsequent water conservation measures, was present in the results most clearly through the addition of more stepped flows after approximately 1997. The stepped shape was often produced when system-wide water storage was prioritized or from recreational flows bordered by power generation (A. Mazurkiewicz, personal communication). Often this shape encompassed a shorter period of power generation from both turbines at Holm Powerhouse, and then a longer period of generation from only a single turbine, potentially indicating a tradeoff between electricity generation and maintenance of water supplies in upstream reservoirs. This flow shape was dominant (explaining 36-37% of the variance) only during the calendar years 2007 and 2009, which were both drier years based on the San Joaquin Valley 5- station Index (CA Department of Water Resources, 2013).

Behaviors of Shapes

Results of the rectangular modeling exercises (Fig. 6) suggest that pulses will show minimal attenuation as they move downstream if the original release is past a certain durational threshold. This concurs with a study by Hauer *et al.* (2012) that found that peak flow reduction is highly dependent on original Q_{\max} duration and original ramping rate. This durational threshold is highly dependent on river morphology as well as Q_{\min} and ΔQ_{tot} . The steep, confined, and relatively monotonous bedrock channel of the Tuolumne River creates conditions in which flood pulses translate downstream rather than attenuate (Magilligan and Nislow, 2005).

The limits to which the Q_{\max} and rising ramping rates decreased were not very different from their original values when the pulses were released. Durational thresholds for common discharges on the Tuolumne River (~3-5 hrs) were comparable to a morning or an afternoon of power generation or the common duration of summer rafting pulses. Within the dataset, 47% of rectangular events and 40% of all events had peak flows lasting greater than 4 hrs long. This suggested that a high percentage of current pulsed flow events were past the durational threshold, and their attenuation reached the limits previously discussed.

The attenuation of the front and back steps differed in key variables. Between representative back step and front step pulses, the back step had less attenuation of the ΔQ_{tot} , but conversely had less steepening of the rising ramping rate. This occurred since the wavefront of the front step pulse had a greater depth gradient, and thus a greater velocity gradient (Sturm, 2001), than that of the back step. The Tuolumne River channel morphology, especially the steep slope, enabled this velocity gradient to cause the wave front to steepen since higher discharges moved downstream with a greater speed. The representative front step pulses had more substantial decreases in Q_{\max} than the back step pulses due to the higher velocity gradient across the peak of the pulse, enabling the peak flows to move forward to overtake the base flows. In both the front and back step pulses, this velocity gradient also caused the portion of the pulse with a higher discharge to move forward and created a long trailing limb with a downramping rate that was lower than the rising ramping rate.

Implications of the Study

The results from this study suggest that mitigation measures are necessary to create a pulsed flow regime that supports aquatic species health. This type of reconciliation will be increasingly necessary under changing hydroclimatic conditions wherein the demands of both native freshwater species (Moyle *et al.* 2013) and river recreation (Ligare *et al.* 2012) will increasingly require coordinated river management. If future management actions followed current practice, operational changes (including ramping rate restrictions) would most likely be devised that minimize harm to focal species (Gostner *et al.* 2011). The disparity between a natural flow regime and that of a hydropeaking river is so drastic that the goals of restricting hydropeaking regimes are often more focused on immediate direct impacts to certain species rather than the restoration of ecological functions (Jones, 2013). In the mainstem Tuolumne River, these focal species could include rainbow trout, sacramento sucker, foothill yellow-legged frogs, and Western pond turtle (McBain and Trush, 2009).

The foothill yellow-legged frog reproductively benefits from a predictable down ramp less than approximately 0.1 meter per week, depending on the river system (Lind and Yarnell, 2011). The effective daily rate to benefit this species is during the window of egg and larval development in the spring, during which stage can currently rise and fall 1m in under 15 minutes directly below Holm Powerhouse. Even for the pulses modeled in this study, the downramping rates of typical pulses after they have attenuated through the entire study reach are ~ 0.1 to 0.3 m per hour, or 168 - 504 x higher than the recommended rate.

This study found that ramping rates for releases would need to be restricted to much lower values for this mitigation measure to be effective as natural attenuation was unable to sufficiently decrease ramping rates downstream to meet the needs of potential focal species.

Although different pulsed shapes did attenuate differently, the ecological benefit from using certain shapes was lessened due to the steep ramping rates that still occurred on the rising and falling limbs. Considering the multiple uses of the water system, including electricity generation and water supply, stringent ramping rate restrictions may not be the most effective mitigation measure for this system or other regulated rivers in the Sierra Nevadas with comparable morphologies. Additionally, the pulsed flow regime may simply be incompatible at certain times with species' needs.

Conclusion

This study demonstrates that natural wave attenuation of flow pulses on the Tuolumne River is not an effective mitigation tool for the sharp changes in discharge caused by hydropeaking throughout the study reach. A large proportion of flow pulses arrive at Don Pedro Reservoir with a similar Q_{\max} and rate of change to the original release conditions. Flow pulse attenuation is highly dependent on Q_{\min} and the shape of the pulse. Furthermore, ramping rates on the rising limb of a pulse flow event can steepen downstream.

The PCA of historic discharge revealed patterns in pulse flow characteristics as a result of management strategies. Although perhaps the predetermined summer recreational flows are the easiest to identify, the study on the whole reveals that within the irregularities associated with hydropeaking operations, operational rules beyond ramping rate policies exist that could potentially be changed depending on stakeholder priorities. A simple example is the

trade-off between front and back step flows and prioritizing either maximum attenuation of Q_{\max} or rising ramping rates.

The Tuolumne River system provides water and electricity to major metropolitan and important agricultural areas, and thus managers and stakeholders will need to balance many conflicting priorities if new environmental measures are implemented. While both operational and structural changes should be considered, knowledge of many contingencies between flow releases and ecosystem responses remains limited or unknown. It will be difficult to address downstream ecosystem consequences of the current regulated flow regime when links between the two are not fully understood. This study provides a basic assessment of the current pulsed flow regime that can be used to support further hydrologic and biologic studies.

Acknowledgements: Thank you to all the denizens at the UC Davis Center for Watershed Sciences, especially Jeff Mount and Bill Fleenor, and Bill Sears and Adam Mazurkiewicz at SFPUC for insights and data. Additional thanks to the USACE for the use of HEC-RAS and USGS for gauge data. This material is based upon work supported by the National Science Foundation Graduate Research Fellowship under Grant No. DGE-1148897. Any opinion, findings, and conclusions or recommendations expressed in this material are those of the authors and do not necessarily reflect the views of the National Science Foundation

References

Bain M. 2007. Hydropower Operations and Environmental Conservation: St. Mary's River, Ontario and Michigan, Canada and USA. International Lake Superior Board of Control.

Barker JD, Sharp MJ and Turner RJ. 2009. Using synchronous fluorescence spectroscopy and principal components analysis to monitor dissolved organic matter dynamics in a glacier system. *Hydrological Processes* 23(10): 1487-1500. DOI: 10.1002/hyp.7274.

Bell E, Kramer S, Zajanc D and Aspittle J. 2008. Salmonid Fry Stranding Mortality Associated with Daily Water Level Fluctuations in Trail Bridge Reservoir, Oregon. *North American Journal of Fisheries Management* 28(5): 1515-1528. DOI: 10.1577/M07-026.1.

Bieri M and Schleiss AJ. 2011. Modelling and Analysis of Hydropeaking in Alpine Catchments equipped with Complex Hydropower Schemes Curran Associates, Inc.: Brisbane, Australia.

Bradford MJ. 1997. An experimental study of stranding of juvenile salmonids on gravel bars and in sidechannels during rapid flow decreases. *Regulated Rivers: Research & Management* 13(5): 395-401. DOI: 10.1002/(SICI)1099-1646(199709/10)13:5<395::AID-RRR464>3.0.CO;2-L.

Bradford MJ, Taylor GC, Allan JA and Higgins PS. 1995. An Experimental Study of the Stranding of Juvenile Coho Salmon and Rainbow Trout during Rapid Flow Decreases under Winter

Conditions. North American Journal of Fisheries Management 15(2): 473-479. DOI:
10.1577/1548-8675(1995)015<0473:AESOTS>2.3.CO;2.

Bruno MC, Maiolini B, Carolli M and Silveri L. 2010. Short time-scale impacts of hydropeaking on benthic invertebrates in an Alpine stream (Trentino, Italy). Limnologica - Ecology and Management of Inland Waters 40(4): 281-290.
DOI:<http://dx.doi.org/10.1016/j.limno.2009.11.012>.

Bruno MC, Siviglia A, Carolli M and Maiolini B. 2012. Multiple drift responses of benthic invertebrates to interacting hydropeaking and thermopeaking waves. Ecohydrology: n/a-n/a.
DOI: 10.1002/eco.1275.

Bunn SE and Arthington AH. 2002. Basic Principles and Ecological Consequences of Altered Flow Regimes for Aquatic Biodiversity. Environmental Management 30(4): 492-507. DOI:
10.1007/s00267-002-2737-0.

California Department of Water Resources and California Cooperative Snow Surveys. 2013. Chronological Reconstructed Sacramento and San Joaquin Valley Water Year Hydrologic Classification Indices, California Data Exchange Center.

Camargo J and Voelz N. 1998. Biotic and Abiotic Changes Along the Recovery Gradient of Two Impounded Rivers with Different Impoundment Use. *Environmental Monitoring and Assessment* 50(2): 143-158. DOI: 10.1023/A:1005712024049.

Campbell KL, Kumar S and Johnson HP. 1972. Stream Straightening Effects on Flood-Runoff Characteristics. *Transactions of the ASAE* 15(1): 94-98.

Cereghino R and Lavandier P. 1998. Influence of hydropeaking on the distribution and larval development of the Plecoptera from a mountain stream. *Regulated Rivers: Research & Management* 14(3): 297-309. DOI: 10.1002/(SICI)1099-1646(199805/06)14:3<297::AID-RRR503>3.0.CO;2-X.

Chow VT. 1959. *Open-Channel Hydraulics*. McGraw-Hill: New York.

Cowx IG, O'Grady KT, Parasiewicz P, Schmutz S and Moog O. 1998. The effect of managed hydropower peaking on the physical habitat, benthos and fish fauna in the River Bregenzerach in Austria. *Fisheries Management and Ecology* 5(5): 403-417. DOI: 10.1046/j.1365-2400.1998.550403.x.

Cushman RM. 1985. Review of Ecological Effects of Rapidly Varying Flows Downstream from Hydroelectric Facilities. *North American Journal of Fisheries Management* 5(3A): 330-339. DOI: 10.1577/1548-8659(1985)5<330:ROEEOR>2.0.CO;2.

Dudgeon D, Arthington AH, Gessner MO, Kawabata Z-I, Knowler DJ, L  v  que C, Naiman RJ, Prieur-Richard A-H, Soto D, Stiassny MJ and Sullivan CA. 2006. Freshwater biodiversity: importance, threats, status and conservation challenges. *Biological Reviews* 81(2): 163-182. DOI: 10.1017/S1464793105006950.

Ferrick MG. 1985. Analysis of River Wave Types. *Water Resources Research* 21(2): 209-220. DOI: 10.1029/WR021i002p00209.

Fette M, Weber C, Peter A and Wehrli B. 2007. Hydropower production and river rehabilitation: A case study on an alpine river. *Environmental Modeling & Assessment* 12(4): 257-267. DOI: 10.1007/s10666-006-9061-7.

Frutiger A. 2004. Ecological impacts of hydroelectric power production on the River Ticino. Part 2: Effects on the larval development of the dominant benthic macroinvertebrate (*Allogamus auricollis*, Trichoptera) *Archiv fur Hydrobiologie* 159(1): 57-75.

Gostner W, Lucarelli C, Theiner D, Kager A, Premstaller G and Schleiss AJ. 2011. A holistic approach to reduce negative impacts of hydropeaking. In *Dams and Reservoirs under Changing Challenges*, (eds). CRC Press. 857-865.

Grant GE, Schmidt JC and Lewis SL. 2013. A Geological Framework for Interpreting Downstream Effects of Dams on Rivers. In *A Peculiar River*, (eds). American Geophysical Union. 203-219.

Halleraker JH, Saltveit SJ, Harby A, Arnekleiv JV, Fjeldstad HP and Kohler B. 2003. Factors influencing stranding of wild juvenile brown trout (*Salmo trutta*) during rapid and frequent flow decreases in an artificial stream. *River Research and Applications* 19(5-6): 589-603. DOI: 10.1002/rra.752.

Hannah DM, Smith BPG, Gurnell AM and McGregor GR. 2000. An approach to hydrograph classification. *Hydrological Processes* 14(2): 317-338. DOI: 10.1002/(SICI)1099-1085(20000215)14:2<317::AID-HYP929>3.0.CO;2-T.

Harby A, Alfredsen K, Fjeldstad HP, Halleraker JH, Arnekleiv JV, Borsányi P, Flodmark LEW, Saltveit SJ, Johansen S, Vehanen T, Huusko A, Clarke K and Scruton D. 2001. Ecological impacts of hydropeaking in rivers. In *Hydropower in the New Millennium, Proceedings of the 4th International Conference on Hydropower Development, Hydropower '01*, Bergen, Norway, 20–22 June 2001., B. Honningsvåg, G. H. Midttomme K. Repp (eds). Balkema. Lisse, Netherlands.

Harby A and Noack M. 2013. Rapid Flow Fluctuations and Impacts on Fish and the Aquatic Ecosystem. In *Ecohydraulics*, (eds). John Wiley & Sons, Ltd. 323-335.

Hauer C, Schober B and Habersack H. 2012. Impact analysis of river morphology and roughness variability on hydropeaking based on numerical modelling. *Hydrological Processes*: n/a-n/a.

DOI: 10.1002/hyp.9519.

Hundley N. 1992. *The Great Thirst: Californians and Water, 1770s - 1990s*. University of California Press: Berkeley and Los Angeles, California.

Jager HI and Bevelhimer MS. 2007. How run-of-river operation affects hydropower generation and value. *Environmental Management* 40(6): 1004-15. DOI: 10.1007/s00267-007-9008-z.

Jayasundara N, Deas M, Tanaka S and Willis A. 2010. Development of a Flow and Temperature Model for the Hetch Hetchy Reach of the Upper Tuolumne River. Prepared for the San Francisco Public Utilities Commission Davis, California.

Jolliffe IT. 2002. *Principal Component Analysis*. Springer-Verlag New York Inc.: New York.

Jones NE. 2013. The dual nature of hydropeaking rivers : Is ecopeaking possible? . *River Research and Applications*: n/a-n/a. DOI: 10.1002/rra.2653.

Jones NE. 2013. The dual nature of hydropeaking rivers : Is ecopeaking possible? . *River Research and Applications*: n/a-n/a. DOI: 10.1002/rra.2653.

Kupferberg SJ, Lind AJ and Palen WJ. 2009. Pulsed Flow Effects on the Foothill Yellow-legged Frog (*Rana boylei*): Population Modeling. California Energy Commission, PIER: Davis, California.

Kupferberg SJ, Lind AJ, Thill V and Yarnell SM. 2011. Water Velocity Tolerance in Tadpoles of the Foothill Yellow-legged Frog (*Rana boylei*): Swimming Performance, Growth, and Survival. *Copeia* 2011(1): 141-152. DOI: 10.1643/CH-10-035.

Le Quesne T, Kendy E and Weston D. 2010. The Implementation Challenge : Taking stock of government policies to protect and restore environmental flows. World Wildlife Fund and The Nature Conservancy.

Ligare ST, Viers JH, Null SE, Rheinheimer DE and Mount JF. 2012. Non-uniform Changes to Whitewater Recreation in California's Sierra Nevada from Regional Climate Warming. *River Research and Applications* 28(8): 1299-1311. DOI: 10.1002/rra.1522.

Lind AJ and Yarnell SM. 2011. Assessment of Risks to Sierra Nevada Populations of Foothill Yellow-Legged Frogs (*Rana boylei*) Under Varying Snow-Melt Hydrograph Recession Rates in Rivers. Placer County Water Agency.

Liu YB, Gebremeskel S, de Smedt F, Hoffmann L and Pfister L. 1999. Simulation of flood reduction by natural river rehabilitation using a distributed hydrological model. *Hydrol. Earth Syst. Sci.* 8(6): 1129-1140. DOI: 10.5194/hess-8-1129-2004.

Lytle DA and Poff NL. 2004. Adaptation to natural flow regimes. *Trends in Ecology & Evolution* 19(2): 94-100. DOI: <http://dx.doi.org/10.1016/j.tree.2003.10.002>.

Magilligan FJ and Nislow K. 2005. Changes in hydrologic regime by dams. *Geomorphology* 71(1-2):61-78.

McBain and Trush. 2009. Upper Tuolumne River Ecosystem Project : O'Shaughnessy Dam Instream Flow Evaluation Study Plan. Prepared for the San Francisco Public Utilities Commission.

Meile T, Boillat JL and Schleiss AJ. 2011. Hydropeaking indicators for characterization of the Upper-Rhone River in Switzerland. *Aquatic Sciences* 73(1): 171-182. DOI: 10.1007/s00027-010-0154-7.

Moog O. 1993. Quantification of daily peak hydropower effects on aquatic fauna and management to minimize environmental impacts. *Regulated Rivers: Research & Management* 8(1-2): 5-14. DOI: 10.1002/rrr.3450080105.

Moriasi D, Arnold J, Van Liew M, Bingner R, Harmel D and Veith T. 2007. Model evaluation guidelines for systematic quantification of accuracy in watershed simulations. *Transactions of the ASABE* 50(3): 885 - 900.

Morrison HA and Smokorowski KE. 2000. The application of various frameworks and models for assessing the effects of hydropeaking on the productivity of aquatic ecosystems. Canadian technical report of fisheries and aquatic sciences no. 2322. Sault Ste. Marie, Ontario.

Moyle PB, Kiernan JD, Crain PK and Quiñones RM. 2013. Climate Change Vulnerability of Native and Alien Freshwater Fishes of California: A Systematic Assessment Approach. PLoS ONE 8(5): e63883. DOI: 10.1371/journal.pone.0063883.

Nagrodski A, Raby GD, Hasler CT, Taylor MK and Cooke SJ. 2012. Fish stranding in freshwater systems: sources, consequences, and mitigation. J Environ Manage 103(133-41. DOI: 10.1016/j.jenvman.2012.03.007.

Nash JE and Sutcliffe JV. 1970. River flow forecasting through conceptual models part I — A discussion of principles. Journal of Hydrology 10(3): 282-290. DOI: [http://dx.doi.org/10.1016/0022-1694\(70\)90255-6](http://dx.doi.org/10.1016/0022-1694(70)90255-6).

Niu S and Insley M. 2013. On the economics of ramping rate restrictions at hydro power plants: Balancing profitability and environmental costs. Energy Economics 39(0): 39-52. DOI: <http://dx.doi.org/10.1016/j.eneco.2013.04.002>.

Null SE and Lund JR. 2006. Reassembling Hetch Hetchy : Water Supply without O'Shaughnessy Dam. JAWRA Journal of the American Water Resources Association 42(2): 395-408. DOI: 10.1111/j.1752-1688.2006.tb03846.x.

Null SE and Viers JH. 2013. In bad waters: Water year classification in nonstationary climates. Water Resources Research 49(2): 1137-1148. DOI: 10.1002/wrcr.20097.

Organisation for Economic Co-operation and Development/International Energy Agency (OECD/IEA). 2010. Renewable Energy Essentials : Hydropower. International Energy Agency.

Person E, Bieri M, Peter A and Schleiss AJ. 2013. Mitigation measures for fish habitat improvement in Alpine rivers affected by hydropower operations. Ecohydrology: n/a-n/a. DOI: 10.1002/eco.1380.

Poff NL, Allan JD, Bain MB, Karr JR, Prestegard KL, Richter BD, Sparks RE and Stromberg JC. 1997. The Natural Flow Regime. BioScience 47(11): 769-784. DOI: 10.2307/1313099.

Saltveit SJ, Halleraker JH, Arnekleiv JV and Harby A. 2001. Field experiments on stranding in juvenile atlantic salmon (*Salmo salar*) and brown trout (*Salmo trutta*) during rapid flow decreases caused by hydropeaking. Regulated Rivers: Research & Management 17(4-5): 609-622. DOI: 10.1002/rrr.652.

San Francisco Planning Department. 2008. Final Program Environmental Impact Report :
Existing Regional Water System. City and County of San Francisco. San Francisco, CA.

Scruton DA, Pennell C, Ollerhead LMN, Alfredsen K, Stickler M, Harby A, Robertson M, Clarke KD
and LeDrew LJ. 2008. A synopsis of 'hydropeaking' studies on the response of juvenile Atlantic
salmon to experimental flow alteration. *Hydrobiologia* 609(1): 263-275. DOI: 10.1007/s10750-
008-9409-x.

Smokorowski KE, Metcalfe RA, Finucan SD, Jones N, Marty J, Power M, Pyrcce RS and Steele R.
2011. Ecosystem level assessment of environmentally based flow restrictions for maintaining
ecosystem integrity: a comparison of a modified peaking versus unaltered river. *Ecohydrology*
4(6): 791-806. DOI: 10.1002/eco.167.

Sturm TW. 2001. Open Channel Hydraulics. McGraw-Hill New York.

Renöfält BM, Jansson R and Nilsson C. 2010. Effects of hydropower generation and
opportunities for environmental flow management in Swedish riverine ecosystems. *Freshwater
Biology* 55(1): 49-67. DOI: 10.1111/j.1365-2427.2009.02241.x.

Richards RR, Gates KK and Kerans BL. 2013. Effects of Simulated Rapid Water Level Fluctuations
(Hydropeaking) on Survival of Sensitive Benthic Species. *River Research and Applications*: n/a-
n/a. DOI: 10.1002/rra.2692.

Richter BD and Thomas GR. 2007. Restoring Environmental Flows by Modifying Dam Operations. *Ecology and Society* 12(1): 12. Available at : <http://www.ecologyandsociety.org/vol12/iss1/art12/>

Rood S, Kalischuk A and Mahoney J. 1998. Initial cottonwood seedling recruitment following the flood of the century of the Oldman River, Alberta, Canada. *Wetlands* 18(4): 557-570. DOI: 10.1007/BF03161672.

Sear DA. 1995. Morphological and sedimentological changes in a gravel-bed river following 12 years of flow regulation for hydropower. *Regulated Rivers: Research & Management* 10(2-4): 247-264. DOI: 10.1002/rrr.3450100219.

Sholtes J and Doyle M. 2010. Effect of Channel Restoration on Flood Wave Attenuation. *Journal of Hydraulic Engineering* 137(2): 196-208. DOI: 10.1061/(ASCE)HY.1943-7900.0000294.

Smokorowski KE, Metcalfe RA, Finucan SD, Jones N, Marty J, Power M, Pyrcce RS and Steele R. 2011. Ecosystem level assessment of environmentally based flow restrictions for maintaining ecosystem integrity: a comparison of a modified peaking versus unaltered river. *Ecohydrology* 4(6): 791-806. DOI: 10.1002/eco.167.

Toffolon M, Siviglia A and Zolezzi G. 2010. Thermal wave dynamics in rivers affected by hydropeaking. *Water Resources Research* 46(8): W08536. DOI: 10.1029/2009WR008234.

Towill Surveying M, and GIS Services. 2007. Survey Report : Tuolumne River Mapping Project. Prepared for the San Francisco Public Utilities Commission and Hetch Hetchy Water and Power.

Troelstrup N, Jr. and Hergenrader G. 1990. Effect of hydropower peaking flow fluctuations on community structure and feeding guilds of invertebrates colonizing artificial substrates in a large impounded river. *Hydrobiologia* 199(3): 217-228. DOI: 10.1007/BF00006354.

Tuhtan J, Noack M and Wieprecht S. 2012. Estimating stranding risk due to hydropeaking for juvenile European grayling considering river morphology. *KSCE Journal of Civil Engineering* 16(2): 197-206. DOI: 10.1007/s12205-012-0002-5.

United States Army Corps of Engineers (USACE). 2010. HEC_RAS River Analysis System : Hydraulic Reference Manual. US Army Corps of Engineers: Davis, CA.

USGS. 2013a. Water-resources data for the United States, Water Year 2012: U.S. Geological Survey Water-Data Report WDR-US-2012, site 11278400, accessed at <http://wdr.water.usgs.gov/wy2012/pdfs/11278400.2012.pdf>

USGS. 2013b. Water-resources data for the United States, Water Year 2012: U.S. Geological Survey Water-Data Report WDR-US-2012, site 11276900, accessed at <http://wdr.water.usgs.gov/wy2012/pdfs/11276900.2012.pdf>

Winter TC, Mallory SE, Allen TR and Rosenberry DO. 2000. The Use of Principal Component Analysis for Interpreting Ground Water Hydrographs. *Ground Water* 38(2): 234-246. DOI: 10.1111/j.1745-6584.2000.tb00335.x.

Yarnell SM, Lind AJ and Mount JF. 2012. Dynamic flow modelling of riverine amphibian habitat with application to regulated flow management. *River Research and Applications* 28(2): 177-191. DOI: 10.1002/rra.1447.

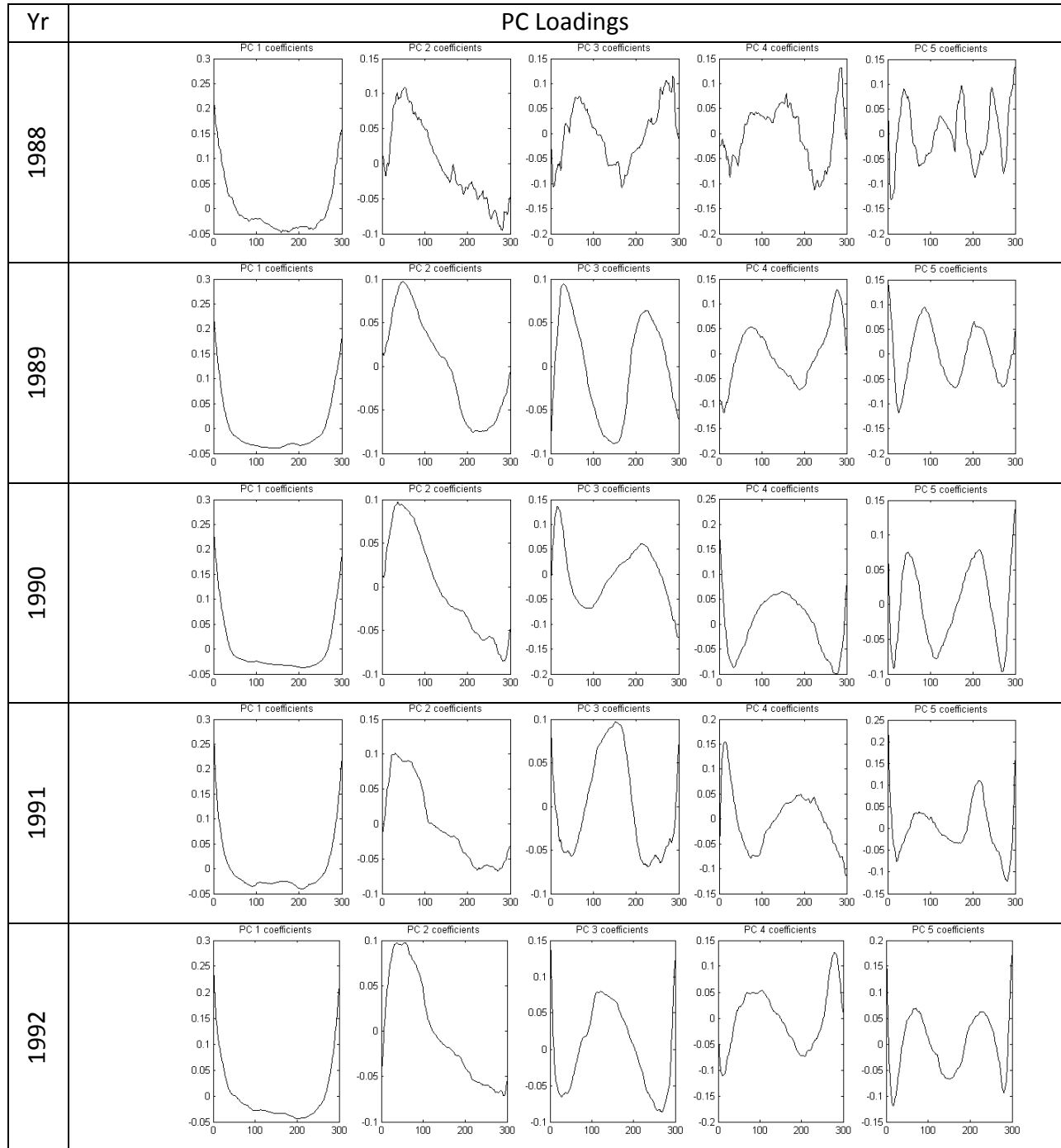
Yarnell SM, Viers JH and Mount JF. 2010. Ecology and Management of the Spring Snowmelt Recession. *BioScience* 60(2): 114-127. DOI: 10.1525/bio.2010.60.2.6.

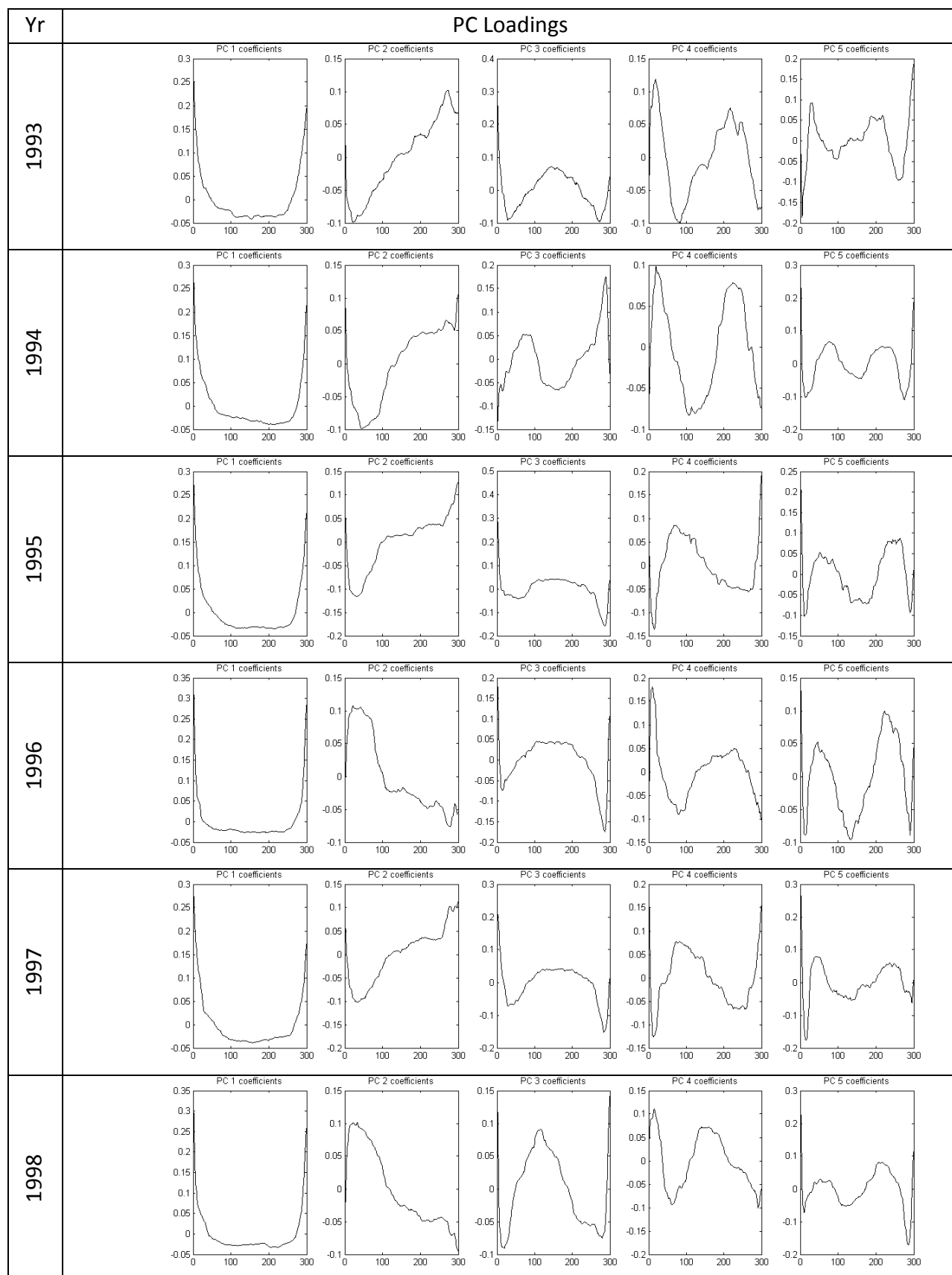
Young P, Cech J, Jr. and Thompson L. 2011. Hydropower-related pulsed-flow impacts on stream fishes: a brief review, conceptual model, knowledge gaps, and research needs. *Reviews in Fish Biology and Fisheries* 21(4): 713-731. DOI: 10.1007/s11160-011-9211-0.

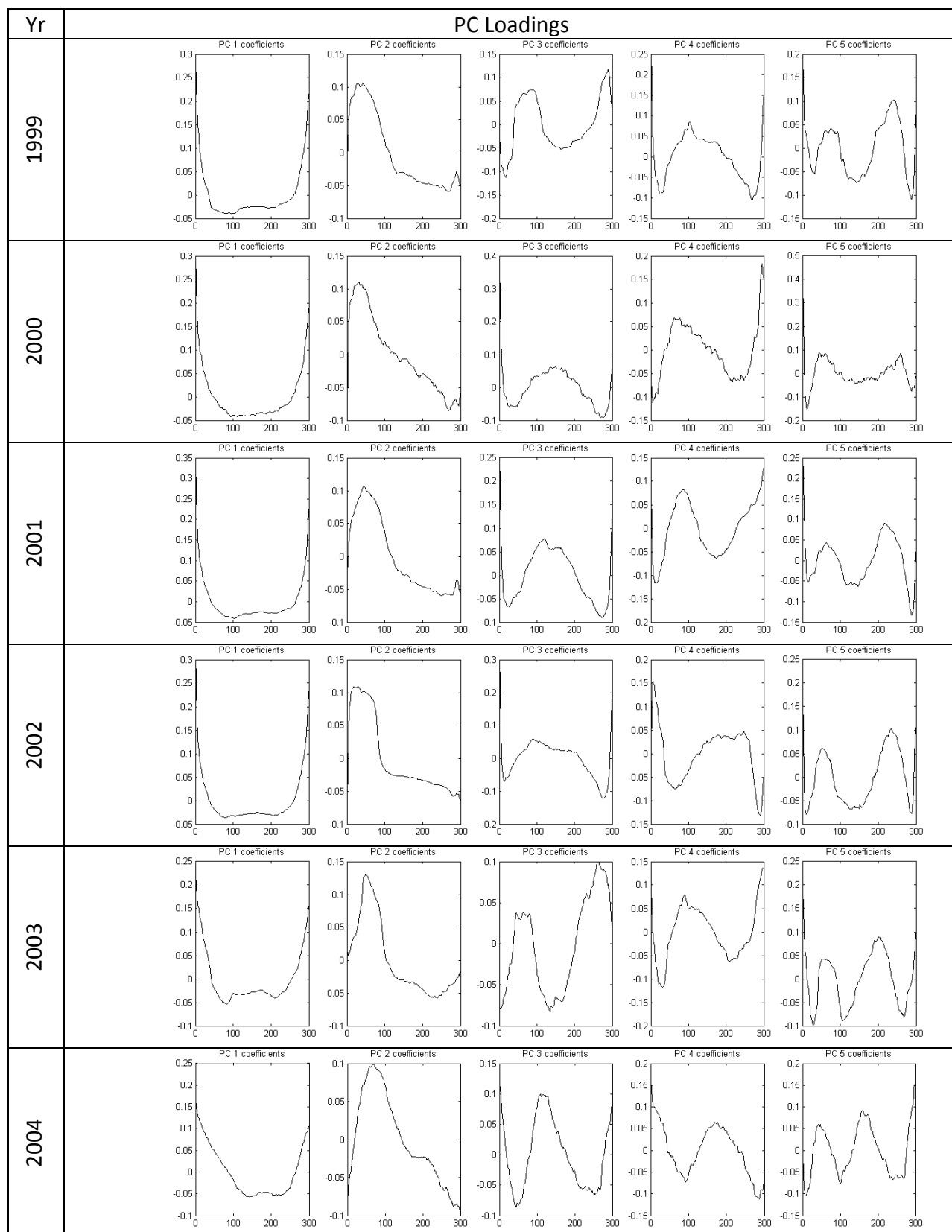
Zolezzi G, Siviglia A, Toffolon M and Maiolini B. 2011. Thermopeak in Alpine streams: event characterization and time scales. *Ecohydrology* 4(4): 564-576. DOI: 10.1002/eco.132.

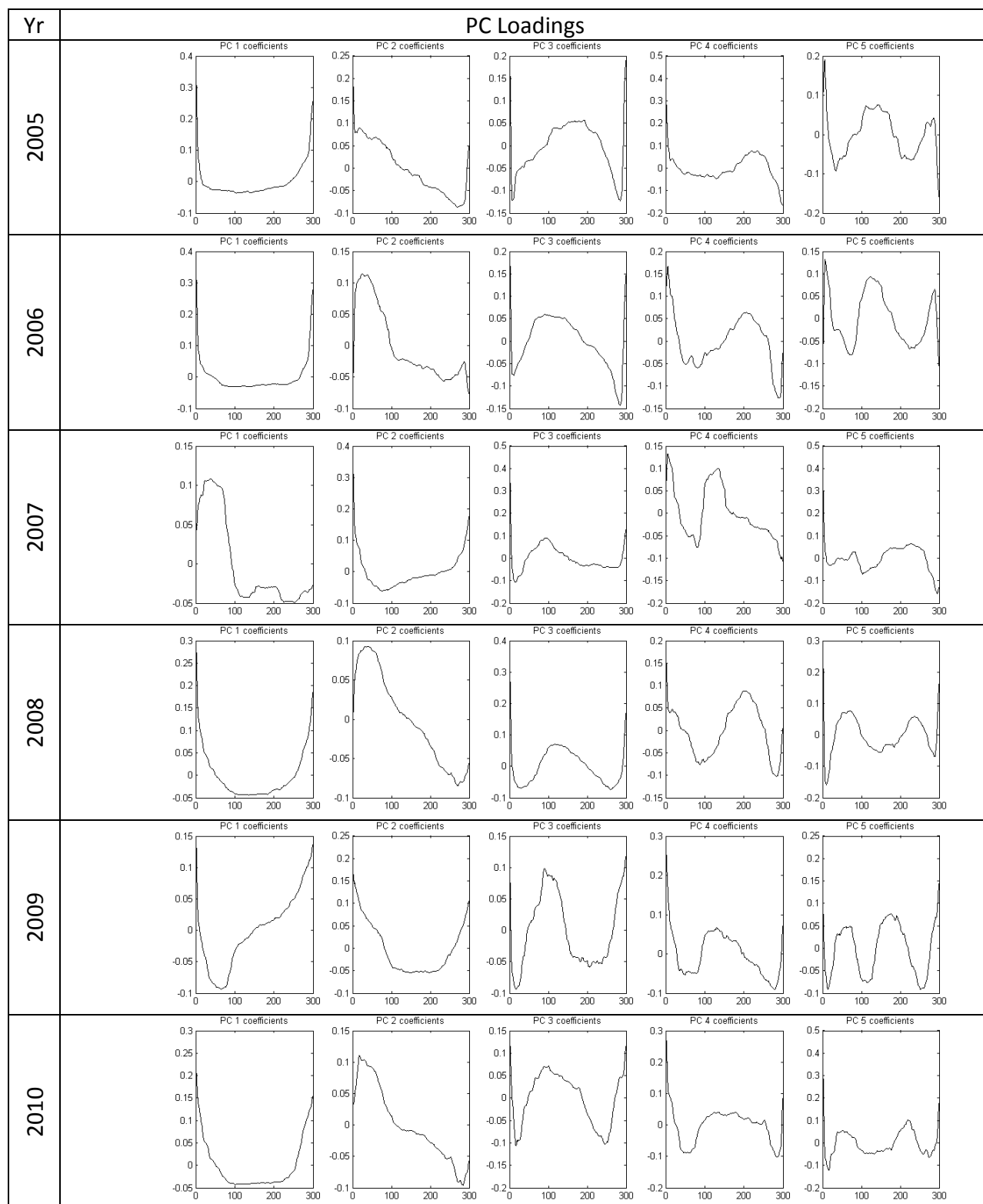
Appendix A

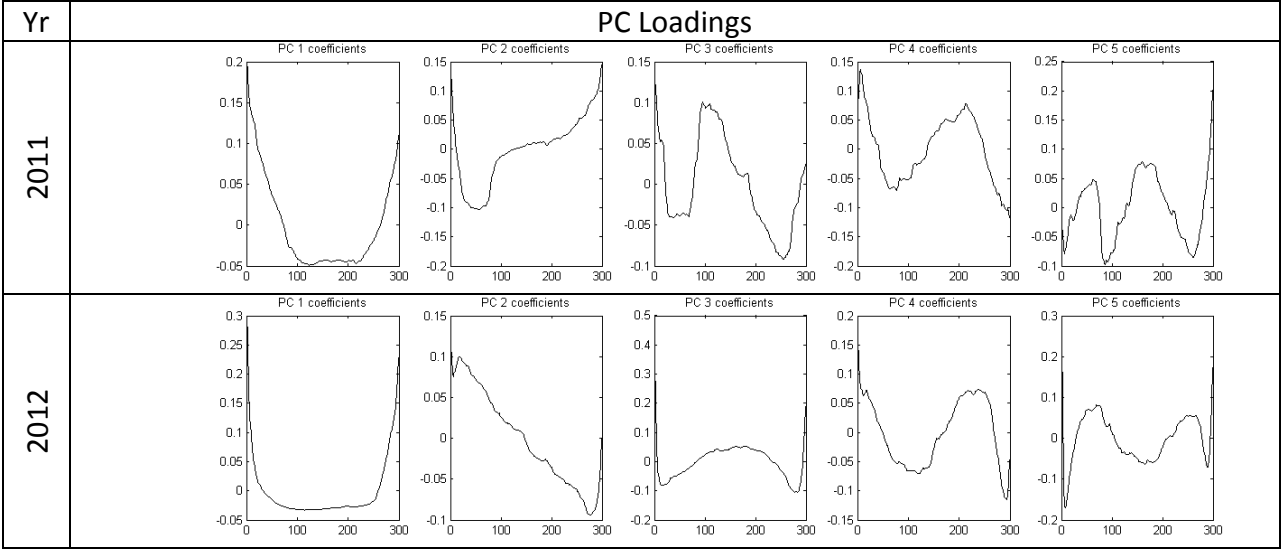
Figure 8 : The following figures represent Principal Component loadings shown by year. Within each year, principal components ordered by % of variance explained. On the x-axis, 0 – 300 was a duration descriptor in which 0 was the beginning and 300 was the end of the event.











Appendix B

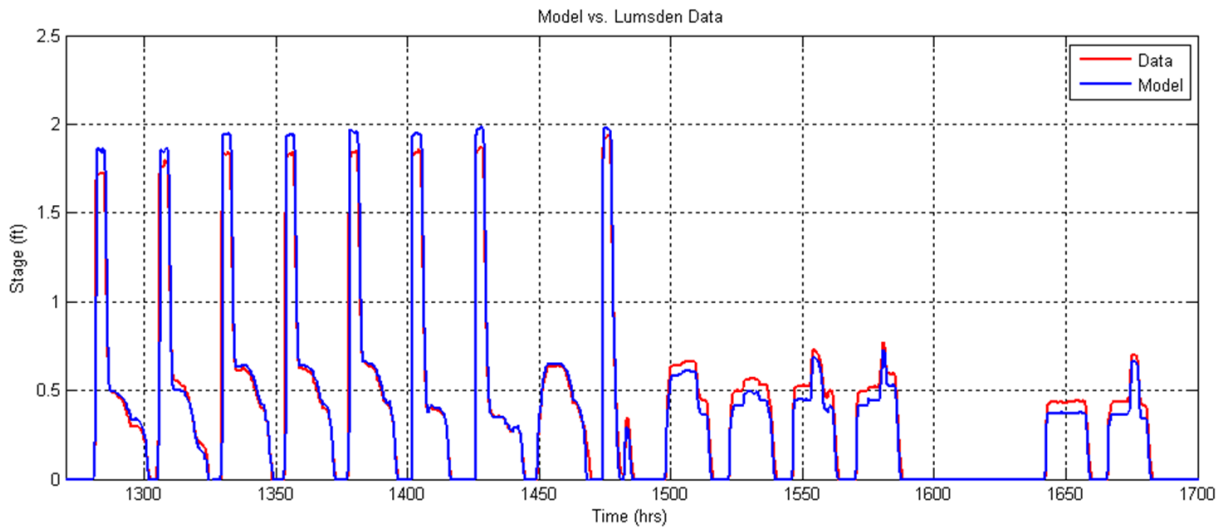


Figure 9 : Further comparison of observed data and modeled data from the validation run. Specifically, a graphical comparison from a portion of the validation time period and a comparison of stage change. Note that the model overpredicts the stage change for pulsed flows released from both turbines, while it underpredicts stage change for smaller releases.

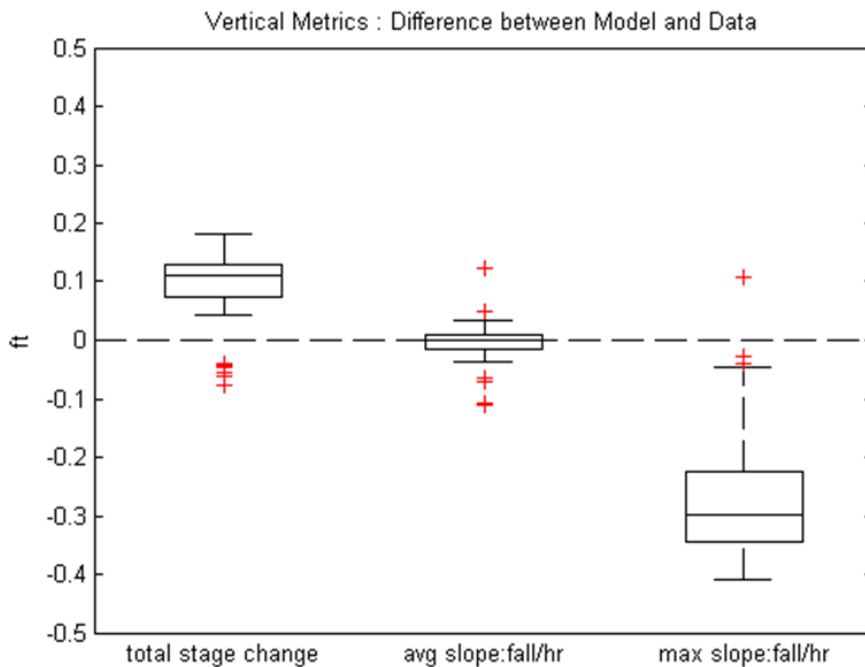


Figure 10 : Comparison of observed data and modeled data from the validation run (stage change and slope of falling limb).

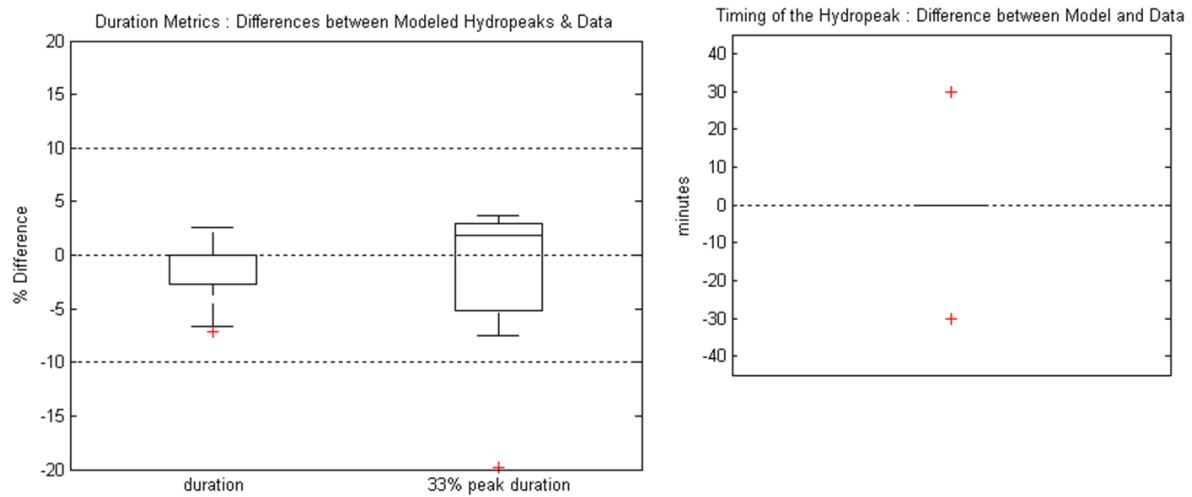


Figure 11 : Comparison of observed data and modeled data from the validation run (duration and time of arrival).